

MICROWAVE PHOTONICS APPROACHES FOR 5G STANDARD

Emilio Ruiz Torregrosa

Supervisor: Beatriz Ortega Tamarit

Trabajo Fin de Grado presentado en la Escuela Técnica Superior de Ingenieros de Telecomunicación de la Universitat Politècnica de València, para la obtención del Título de Graduado en Ingeniería de Tecnologías y Servicios de Telecomunicación

Curso 2016-17

Valencia, 12 de septiembre de 2017

Resumen

El propósito de este Trabajo Fin de Grado es el de presentar diversos sistemas para la generación de señales de microondas mediante la utilización de técnicas de fotónica de microondas con el fin de ser empleadas en el nuevo estándar 5G. Para la simulación se ha empleado el software de simulación VPI photonics. Todos los diseños se basan en el uso de un modulador Mach-Zehnder polarizado en el punto de mínima transmisión para generar la señal. Un diseño basado en este método es empleado para transmitir datos NRZ OOK a 10 Gbps sobre una señal a 30 GHz a partir de un oscilador que emite una señal de 15 GHz. El sistema es comparado con uno que no emplea técnicas de fotónica de microondas dando un buen resultado tanto en comportamiento como en coste. Asimismo, se presentan otras alternativas que utilizan la dispersión estimulada de Brillouin (SBS) para incrementar la frecuencia de la portadora sin aumentar la frecuencia del oscilador. Por último, se demuestra un esquema que también hace uso del SBS para generar pulsos triangulares a 5, 8 y 10 GHz; y un esquema que emplea dos láseres consiguiendo una mayor flexibilidad en la sintonización.

Resum

El propòsit d'aquest Treball Fi de Grau és el de presentar diversos sistemes per a la generació de senyals de microones per mitjà de la utilització de tècniques de fotònica de microones amb l'objectiu de ser utilitzades en el nou estàndard 5G. Per a la simulació s'ha disposat del programari de simulació VPI photonics. Tots els dissenys es basen en l'ús d'un modulador Mach-Zehnder polaritzat en el punt de mínima transmissió per a generar el senyal. Un disseny basat en este mètode és empleat per a transmetre dades NRZ OOK a 10 Gbps sobre un senyal a 30 GHz a partir d'un oscil·lador que emet un senyal de 15 GHz. El sistema es compara amb un que no empra tècniques de fotònica de microones donant un bon resultat tant en comportament com en cost. Així mateix es presenten altres alternatives que utilitzen la dispersió estimulada de Brillouin (SBS) per a incrementar la freqüència de la portadora sense augmentar la freqüència de l'oscil·lador. Finalment, es demostra un esquema que també fa ús del SBS per a generar pulsos triangulars a 5, 8 i 10 GHz; i un esquema que empra dos làsers aconseguint una major flexibilitat en la sintonització.

Abstract

The aim of this Final Degree Thesis is to present diverse systems for the generation of microwave signals through the utilization of microwave photonic techniques with the intention of being employed in the new standard 5G. For the simulation work, VPI photonics simulation platform software has been utilized. All the designs are based on the use of a Mach-Zehnder modulator biased at the minimum transmission point to generate the signal. A design based on this method is employed to transmit NRZ OOK data at 10 Gbps over a 30 GHz signal by an oscillator which beams a 15 GHz signal. The system is compared with one which does not make use of microwave photonic techniques giving a satisfactory result both in the behavior and the cost. Additionally, other alternatives that utilize the Stimulated Brillouin Scattering (SBS) to increment the carrier frequency without increasing the oscillator frequency are presented. Lastly, a scheme that also make use of SBS is demonstrated to be able to generate triangular-shaped pulses at 5,8 and 10 GHz; and a design with two lasers is also demonstrated, achieving an enhanced flexibility in the tunability.

INDEX

Chapter 1. Introduction	4
1.1 Motivation.....	4
1.2 Objectives.....	4
1.3 Structure	5
Chapter 2. The future standard 5G.....	6
2.1 Network architecture	7
2.2 Technology.....	9
2.3 Frequency bands.....	12
2.4 Transmission Standards.....	15
Chapter 3. The role of microwave photonics	18
3.1 Radio-over-Fiber (RoF) Transmission	19
3.1.1 Figures of Merit and RoF Link Limitations	19
3.1.2 RoF role in Virtualized RAN	20
3.2 Indoor Frequency Up-Conversion RoF Link	20
3.3 RF Signal Photonic Generation.....	22
3.4 Optical Conformation.....	26
3.5 Filtering	27
Chapter 4. System Designs, Simulations and Results	30
4.1 Description of the Software.....	31
4.2 Conventional 10 Gbps NRZ OOK RoF Link.....	34
4.3 Microwave Photonics based 10 Gbps NRZ OOK RoF Link	40
4.4 Optical microwave generator based on SBS with fine tunability.....	44
4.5 Photonic generation of triangular-shaped microwave pulses using SBS-based optical carrier processing	48
4.6 Flexible two lasers RF mm-wave generation system.....	52
Chapter 5. Budget.....	55
Chapter 6. Conclusions and Future Lines	58
6.1 Conclusions	58
6.2 Future Lines	59
References.....	60

Chapter 1. Introduction

1.1 Motivation

Nowadays, each time more and more devices are being connected to internet, and the predictions talk about a vast number of connected devices in the near future. Not only mobile phones, tablets, computers or wearables but also household appliances. It is becoming common to have more 'intelligent' white goods that can be turned on/off without being at home. Future technologies planned as the vehicle-to-vehicle communication, or the increasing requirements in terms of bandwidth, data rate and even latency force to look for an improvement of the current network.

5G is described as the next generation mobile network, however, it is not projected as a modest improvement over 4G but as an almost completely new network. Therefore, recurrent researches are carried out to construct the new generation network, which is still immature.

5G has some challenges that must be overcome. Multiple antennas per device will be common, so the beamforming and steering is very important to enhance the performance, the efficiency and reduce the interferences. New frequencies must be dedicated as the currents are very saturated. Studies talk about employing higher frequencies, in the range of microwaves. Besides, is very important to improve the efficiency.

To beat some issues, microwave photonics is presented as a key technology. This versatile field is being studied in many researches as the pillar of processes as optical conformation, filtering or RF signal generation.

In this way, the interest of satisfying the future needs and the promising application of microwave photonic techniques are the main source of motivation to develop this thesis.

1.2 Objectives

The objective of this thesis is the study of different RF mm-wave signal generation systems by using microwave photonic techniques with a view to the next generation mobile network (5G). To achieve this aim, some goals are defined:

- Study and selection of the network architectures proposed, the frequency bands of interest and the key technologies, in order to know the likely path 5G will follow.
- Gather the present transmission standards to have a vision of the state of maturity of the network.
- Define the Radio-over-transmission, discover the main problems of this kind of links and introduce some indoor networks based on these links.
- Study the potential applications of microwave photonic techniques inside the new standard.
- Search and investigation of possible designs to generate RF mm-wave signals.
- Learn the basics of VPI photonics, the simulation platform software employed.

- Simulate and analyze the viability of the proposed generator systems.
- Estimate the budget of implementing the systems simulated in order to be able to compare them in economic terms.

1.3 Structure

The thesis is structured in six chapters. The first chapter introduces the motivation to realize the thesis, as well as its objectives and structure. Throughout the second chapter, the 5G network is studied. A list of recommended frequency bands is analyzed and, the network architecture, its technology and transmission standards are commented.

The next chapter discuss about Radio-over-fiber transmission and different microwave photonic techniques are presented to supply important processes inside the future network as RF mm-wave signal generation.

Once the theoretical background is explained, is the turn to show the work realized: the simulation of different RF mm-wave generator systems.

In chapter 5 an estimated budget of implementing the different systems is disaggregated in order to compare the designs in economic terms

The last chapter gather the conclusions and future investigation lines. Finally, references complete the thesis.

Chapter 2. The future standard 5G

This thesis focuses on the study of the role of the Microwave Photonics in a 5G indoor network. In order to perform any assessment, it is necessary to have a deep knowledge of the system under study. Therefore, the system depends on two fundamental pillars: 5G standard and microwave photonics. This chapter provides the required information in terms of the 5G standard.

Although the standard is yet under study, there are many researches which agree in several aspects of the new technology, and they are presented in this thesis. However, it is remarkable that new or edited requirements in the future could be defined.

The chapter has been divided into the next sections:

- Section 2.1 describes Network architecture
- Section 2.2 presents the Technology
- Section 2.3 describes the recommended Frequency bands
- Section 2.4 introduces the Transmission Standards

2.1 Network architecture

In order to support the increasingly data rates, the massive number of devices, the lower latencies; and to manage the volume of new spectrum (primarily on higher bands) of the 5G network is necessary a completely new architecture.

Virtualization is a promising technology. With a view to face some of the main challenges of deploying new services, network operators started to work with Virtual Network Functions (VNFs). These functions can implement network functions traditionally implemented via custom hardware appliances and middleboxes. These could be located either in data centers, network nodes or at end user premises. The basic idea is to execute RAN functionality on more generic and generally available execution hardware and software platform. However, some network functions have such strong timing relations with the radio, or depend so strongly that it is challenging to virtualize them. The question now is: which parts of the RAN are viable to be executed on a virtualized environment?

Another concept more and more present in 5G is Network Slices. A wide variety of services, requirements and scenarios is a main feature in 5G networks. Network slicing will help the operators to address these different use cases efficiently. The idea consists in deploying multiple logical networks as independent, but using a common physical infrastructure. In this common infrastructure, the physical network resources are separated from the logical network through Virtual Network Functions and Software Defined Networking (SDN). A 5G slice could be composed of a collection of 5G network functions (NF) and specific radio access technology (RAT) settings that are combined for a specific use case.

Currently, 4G networks have been deployed making use of Distributed and Centralized RAN. In a D-RAN all processing is performed locally at the access point (AP) while in a C-RAN all processing is allocated to a central unit (CU). This Central Unit serves multiple distributed radio sites, and the transmission link between it and the radio units use CPRI fronthaul over dedicated fiber or microwave links. However, the introduction of high bandwidth layers' forces to redesign the RAN architecture. Virtualized RAN exploits the throughput capabilities and limited coverage of the new spectrum. The Virtualized RAN architecture leverages NFV techniques and data center processing capabilities and enables coordination and centralization in mobile networks. It supports cost-efficient processor sharing, scalability, layer interworking and robust mobility.

There is consensus that 5G logical architecture should foresee a split of control and user planes. Virtualized RAN allows to realize it enabling individual scalability of both planes and logical centralized control.

Within the RAN, different considerations on possible function splits are being pursued (Figure 1):

1. **Function split within PHY layer.** Its main disadvantage is that the bandwidth requirements on the fronthaul interface scale with the number of antennas.
2. **Function split between PHY and MAC (alternative 1).** The advantage is the lower resulting fronthaul rates, but only MAC-level functions would be centralized.
3. **Function split between synchronous and asynchronous functions (alternative 2).** It enables multi-connectivity, exploits eventual pooling gains.

Whatever the functional split point is defined, it is essential that the architecture ideally supports all the possibilities by leveraging on generic interfaces with varying degrees of traffic multiplexing and/or routing capabilities.

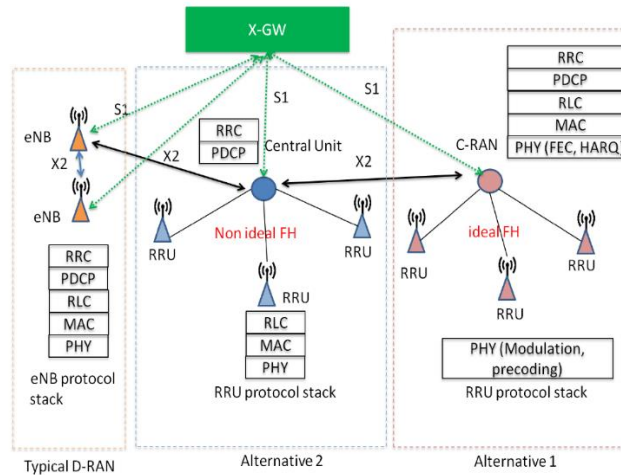


Figure 1. Possible function splits in the RAN.

Indoor Architecture. As 5G is expected to employ mmWave frequencies, it is necessary to differentiate between indoor and outdoor networks in 5G since the propagation loss through buildings at these frequencies is very severe.

Although the different technologies mentioned would be able to provide multi-Gb/s Wireless access, backhaul connectivity to every dwelling is a major challenge. There are two options: (1) PON based on FTTx technologies and (2) mmWave band backhaul. Passive optical networks based on fibre is very extended. However, laying down optical fibre to each housing is expensive in some cases. Point to point backhaul connectivity offers highly flexible, cost efficient and rapid deployment of multi-Gb/s connectivity. On the other hand, ensuring line-of-sight in case of mmWave backhauling is difficult in some scenarios.

The architecture referred previously highlights the use of a central unit to manage the network. Besides, the architecture must define a common infrastructure where the central processor handles the processing operations leveraging the VNFs. To perform the architecture described in an indoor scenario, micro C-RAN (mCRAN) architecture has been proposed. It employs 60 GHz frequency band for high speed indoor communication and RoF technology to enable centralized base-band processing. Due to the high path loss and the limitation to diffract around obstacles of the frequency band multiple mmWave APs would be required to cover indoor areas. Every room becomes a separate 60 GHz cell, therefore frequent handovers can be unchained. To make network management easy, centrally managed network architecture with simple access points is desirable.

Figure 2 shows the diagram of the outlined architecture. Centralized Home Communication Controller (HCC) is responsible for radio access control, signal generation, distribution and processing. Each room has at least one Radio Access Point (RAPs) with radio beam-steering controlled by the HCC. The connection between the HCC and the RAPs is realized through optical fibre via the Reconfiguration Nodes (RNs). Depending on HCC's instructions, the RN and RAP perform routing/reconfigurable bandwidth allocation and beam-steering, OE/EO-Conversion, respectively. The RN is a remote process unit whose responsibility is to configure the RAP.

From HCC to RAP it is necessary to count on separate control channels for beamforming mechanism in synchronization with the data channel. For short range communications at 60 GHz IEEE 802.11 ad has proposed threes PHYs: Control PHY (27.5Mbps), SC PHY and OFDM PHY (7 Gb/s). Timing in IEEE 82.11 ad is based on beacons intervals. Inside a beacon interval we find different access periods having different medium access rules (CSMA/CA and TDMA).

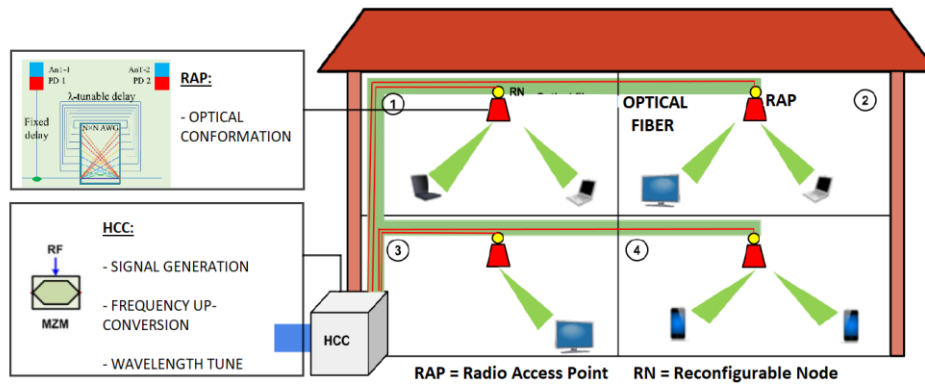


Figure 2. A schematic of mCRAN architecture

2.2 Technology

The 5G cellular network is still being designed and its future key features are being investigated. Despite of the uncertainty, the use cases and requirements have already been defined, and they show that the future cellular network will not be a simple evolution of the current system. Within the framework of achieving these specifications, the R&D industry has identified several disruptive technologies which will be key.

The small cells incorporation, the use of the millimeter-Wave spectrum, explained in section 2.3, and realizing massive MIMO are the three fundamental pillars which will support the new network. Besides, microwave photonics will be essential to create the 5G network.

In addition to these technologies, experts have found some common trends and promising technologies for building up the next generation: flexible duplex, self-backhauling, direct device-to-device communication, Radio-over-fiber (explained in section 0), Multi-RAT and ultra-lean design.

2.2.1 Massive MIMO and Small Cells

Multiple-input-multiple-output (MIMO) technology consists on the transmission and reception through more than one antenna. It takes the advantage of multiple antennas at transmitter and/or receiver so the network throughput, capacity and coverage can be improved without additional bandwidth or transmit power level. Recent advances have led the change from single user MIMO to multiuser MIMO (MU-MIMO) as hosting several antennas in a mobile terminal is challenging. This system is based on a base station with multiple antennas that serves a bunch of single or multiple antennas users simultaneously. Some current networks use a somewhat low-order version of MIMO.

Small cells principle is based on cell densification by reducing the cells size. Small cells enable better frequency reuse and, energy and cost reductions. Moreover, high frequency bands will be essential in the new standard as illustrated in section 2.3. At these frequencies, the path losses are so high that the coverage is reduced. Therefore, small cells fit very well with the new frequency bands by reducing the area to cover by the base station.

Besides, the high path losses require coverage-enhancing solutions. Transmitting and receiving multiple data streams in a user equipment could overcome the issues related to the path losses. Along with massive MIMO, the research is focused on dynamically steering the beam to the user devices (beamforming, section 3.4). Instead of transmitting in all directions, directional antennas confine signal power in a direction. Then, the amount of signal received by a user is increased and the interferences between antennas can be reduced, so the energy consumption is improved as the same amount of signal received power is achieved with less transmission power.

High frequency bands are more attractive for Massive MIMO deployment because, to avoid spatial correlation and antenna mutual coupling in a multiple antenna structure, antennas

must be spaced at least the half wavelength of the radio signal. At millimeter-wave, the number of antenna elements in the access points could be even more than 1000.

On this basis, it could be claimed that small cells, mm-Wave spectrum and massive MIMO fit perfectly. In [1], the feasibility to combine small cells and Massive MIMO is studied. 2D antenna array system (AAS) presents similar coverage but additional high SINR region in low density small cell case to that of omnidirectional antenna. In high density case, the 2D AAS obtains much better coverage due to the amount of ICI introduced by the omnidirectional antenna. In [2], a 3D-MIMO design is proposed. The structure is composed with 128 antenna elements and is designed to work at 2.6 GHz frequency band. Moreover, field trials are performed showing that it can help 5G to achieve the spectral efficiency target.

2.2.2 Flexible Duplex

Since the beginning of mobile communication, Frequency Division Duplex (FDD) has become the dominant network duplex technology because the most popular service in mobile networks requires symmetrical traffic loads for DL and UL. Inside the 5G goals we can find the dynamic asymmetric resource provision between up- and downstream traffic. In comparison with FDD, Time Division Duplex (TDD) benefit the system with more flexibility to adapt time-domain resources with ratio between UL and DL traffics, lower hardware cost and the unpaired band allocation. However, not all are advantages and some challenging issues have been identified.

The trend for duplex technology in the next generation will be the convergence of FDD and TDD in what is called flexible duplex[3]. Furthermore, in established TDD network the same DL/UL subframe configuration is adopted to avoid inter-cell interference between UL and DL signals. With flexible duplex, any subframe may either be allocated for UL and DL transmission for a certain cell in a dynamic way. This leads to an improved system throughput.

In conclusion, FDD will remain the main duplex scheme for lower frequencies and long cover areas whereas TDD is a better choice in small cells, asymmetric traffic and unpaired spectrum case[4].

2.2.3 Self-Backhauling

Backhaul connectivity could be realized via wireless or wired technology. In the context of 5G cellular network, a fundamental challenge is to provide an economical and ubiquitous backhaul connectivity to these small cells. As the access link will extend to higher frequencies, access and backhaul will share the same wireless channel (self-backhauling).

This enables efficient usage of frequency resources, higher cost efficiency and higher performance. However, it induces additional interference, complex scheduling of the channel resources and potential limitation on the end user experience due to the sharing of resources. Research in this area is being realized to discover the challenges, solutions and possibilities of this technology[5], [6]. An option to avoid or reduce the new interferences is the use of interference management strategy as proposed in [7].

2.2.4 Direct Device-to-Device Communication

Device-to-device (D2D) communication commonly refers to a kind of technology that enables direct communication between devices without communication infrastructures[8]. With the accelerating growth of Machine-to-Machine (M2M) applications, D2D is being accepted as a part of the fourth generation. In the 5G era, D2D communications should be a part of the overall wireless-access solution. It is expected to provide, not only peer-to-peer user-data direct communication, but also network coverage expansion using mobile devices.

It presents a variety of challenges as the efficiently radio resources reallocation among cellular and D2D users, and the prevention or control of the interferences inside the cellular system. Several studies ([9], [10]) analyze diverse ways to try to overcome these issues. Moreover, energy efficiency is a key objective as the battery in mobile devices is limited. In [11], a study of D2D transmission for use in 5G cellular networks shows that this scheme is more effective in regards to power and connection efficiency. It improves the system throughput and can reduce the traffic loads.

2.2.5 Multi-Radio Access Technology (Multi-RAT)

The fifth generation will suppose a substantial twist from the current networks. For 5G two RAT options can be foreseen. On the one hand, we find a single unified RAT with such flexibility that can be optimized for different frequencies and use cases through parameter configuration. This flexibility is still technically challenging, and the maturity of LTE/LTE-A could make economically inviable the new RAT deployment. To solve these inconvenient, the other possibility is the utilization of multiple RATs, each of them with a different air interface, which complement each other acting as a single unit. It seems technically easier to achieve and more economically viable.

5G will be encompassed by more than one RAT, each optimized for certain use cases and/or spectrum. The number of RATs should be minimized. In [12], three interfacing options for the access technologies are introduced (Figure 3).

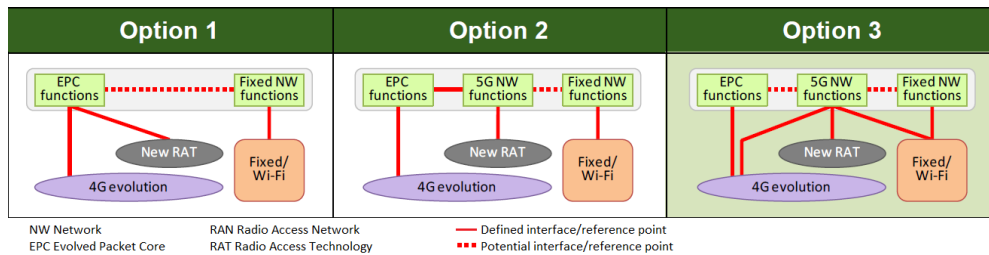


Figure 3. Access-technology interfacing options

In the first option, EPC provides all access components supporting the 5G RAT family. This makes necessary an evolution of EPC to enable the new 5G access functions. The impact on traditional RAN is minimum, however, legacy paradigms may be applied to all use cases with its corresponding inefficiency and higher cost.

The second option is based on an evolved EPC and a new design referred to as “5G NW functions”. Both support the new 5G access functions, nevertheless, only the new design endures the new RAT. The other RAT (4G evolution) is supported by the EPC. This option benefits from new technologies with a minimal impact to legacy RAN. Nonetheless, the new design could only be utilized where there is new RAT coverage and, because of the limited coverage of the new RAT, it is crucial to support mobility between new RAT and 4G evolution, incurring in signaling burden.

NGMN describes the third one as the most interesting option. In the design, all the 5G RAT family components, the other RATs and even the fixed network are supported by the new 5G Network Functions (5GFs) design. It also provides backward compatibility with devices which cannot use the new design by supporting the 4G evolution through the EPC. As option 2, it allows the benefits from new technologies, but overcomes the mobility issues since the 5G NW functions handle the new RAT and 4G evolution. Even in areas without new RAT coverage, all RATs can immediately benefit from the 5GFs. However, some issues should be considered: 4G should be upgraded to support connection through the EPC and the new 5GFs, and the potential impact on legacy RAN to operate concurrently with legacy core network (CN) functions and 5G NW functions.

2.2.6 Ultra-lean Design

The basic principle is to minimize any transmission not directly related to the user data delivery. These include signals for synchronization, idle-mode mobility and system and control information [13]. The design enables higher data rates by reducing interference from non-user data related transmissions. Moreover, it improves the energy performance as it enables network nodes to stay at low-energy states in longer situations.

In [14], the energy performance of 5G RAT systems characterized by ultra-lean design and massive beamforming is evaluated and compared with an LTE system in a dense urban scenario. A decreased energy consumption of more than 50% is expected from 2020. Lean transmission is important for all kinds of deployments, although especially for the dense one.

2.3 Frequency bands

The radio spectrum is a limited resource that must be efficiently exploited. Although the 5G standard specifications are not definitely defined yet, it exists a consensus around the utilization of the millimeter-wave (mmWave) spectrum as one of the 5G fundamental pillars [15], [16]. In the LTE standard, all the frequency bands employed are lower than 6 GHz. 2100, 1800, 2600, 800, 700 and 2300 MHz frequency bands are the most common around the world.

Nowadays, spectrum below 1 GHz has already a very intensive use. Moreover, it is well accepted by the industry that an order of 1 GHz bandwidth per operator will be necessary, although 500 MHz could be considered if really needed [17]. Therefore, it is evident that the 5G standard will have to resort to spectrum bands above 6 GHz, to which we will referred as ‘mmW’ from now on. The main idea is to continue utilizing frequency bands around the 4G bands, overall in macrocell outdoor scenarios, while spectrum bands above 6 GHz will provide high data rate, overall in microcell indoor scenarios.

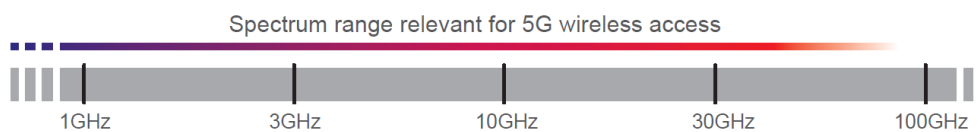


Figure 4. Spectrum relevant for 5G wireless access

The range below 30 GHz is preferred due to its propagation properties, but the higher range has larger amounts of spectrum and possibilities wide transmission frequency bands. Then, high frequencies (especially above 10 GHz) serve as a complement (additional capacity and/or extreme data rates) to lower frequency bands, which will also remain the backbone for mobile-communications in 5G. Contiguous bands are preferred to avoid additional complexity, although individual bands in a multi-operator environment could be separated but close enough to have similar propagation conditions.

Propagation at these high-frequencies is highly directional and the coverage mechanism is by line-of-sight or via multiple reflections. The penetration capability is very poor due to the losses. The combination of mmW and small-cells solve the reach limitation by reducing the coverage area of every cell. Neither fundamental nor technology limitations determinate the bands priority from 6 to 100 GHz. This is because at short distances, of the order of 200 m, fundamental are not a limiting factor up to at least 100 GHz and the technologies required will be soon available.

The main challenge in the frequency bands election is global spectrum availability so the usage is globally harmonized.

In [18] a spectrum analysis is realized from a UK/European point of view. The analysis split the spectrum into separate ranges: 6-30 GHz, 30-100 GHz and over 100 GHz, based on the characteristics of the spectrum use in each range.

5-30 GHz band. In this range is difficult to find bandwidths of several GHz. An attraction is the little development required to employ the existing cellular technology and architecture.

There is strong interest from the satellite industry as well as for the fixed service. Sharing with both industries is likely to be challenging and would offer limited bandwidth. The band identified above 30 GHz has greater bandwidth and less sharing issues. Despite, there is a strong interest in 28 GHz band from the USA, Korea and Japan the ITU-R has not proposed it as a need for study band before WRC-19[19].

30-100 GHz band. Passive, fixed, MoD and collective use dominate this band. Besides, the exclusive civil bands are too small for independent 5G mmW use.

There is more bandwidth available than in lower ranges, with potentially more sparse coexistence concerns. In this range, we found the band 60 GHz with an oxygen absorption peak within which WiGig systems have been developed, and the 70/80 GHz bands. The lasts may be attractive since the same operators might wish to operate access and backhaul in-band and to handle the coordination challenges themselves.

The most important bands are the following:

- **The 66-71GHz band** has a mobile allocation which is unused. The band is wide and close to the WiGig band, therefore low-cost technology should be available. Although, no use is known, it is also allocated to GNSS and ISS. Then collective use is proposed, as at higher frequencies the probability of interference decrease.

Furthermore, this band is allocated to mobile in at least Europe, China, Japan, South Korea and USA.

- **The 45.4-48.9 GHz band** includes two relatively small exclusive bands used for the Amateur service and PMSE. The PMSE band may be suitable for removal since no allocations were made, but the Amateur service has a clear usage. Nevertheless, avoiding these bands there is still 2.8 GHz available non-contiguously.

45.5-47 GHz is allocated to RNSS but unused. Vodafone has suggested the wider range 43-47 GHz could be considered for 5G mmW, however, 43.5-45.5 GHz is an harmonised NATO band, with potential for future mobile use. As the previous band, these bands could also be suitable for collective use.

- **The 40.5-43.5 band** is the concatenation of two bands where the 40.5-42.5 GHz portion has no primary mobile allocation in Europe. Despite this, the low usage opened it to the fixed service. Anyhow it continues to be low used, so it could be reconsidered for 5G mmW access.

- **The 71-76 and 81-86GHz** are typically light licensed bands, but they are relatively suitable for backhaul. Point-to-point fixed links is their global main usage. Interference could appear between 5G backhaul and the access networks for the users so a frequency plan would be needed. Operators might want to self-coordinate between their own access and backhaul networks in portions of this band.

- **The 57-66 GHz license exempt band** has spurred the creation of the Wi-Fi Alliance's WiGig. This allocation is available globally, but 5G mmW could enter this band directly via collective use. However, the power/antenna limits may need to be re-assessed for outdoor operation at 200m.

Above 100 GHz band. This band contains several water and oxygen absorption peaks. This range remains of interest because of the huge bandwidths which are possible. Although it would be appropriate due to its disuse, pre-existing allocations should be respected. Over the next 5 years this band may be best suited for backhaul as the cost point of backhaul best supports the specialized technology required.

There are many unavailable passive bands, and much of the remainder is allocated to the Radio Astronomy Service. The residual bands have the potential to support backhaul for 5G mmW but its range will be limited by atmospheric. Besides, maybe there is already enough fixed link spectrum.

Freq Band	Usage known	Pros	Cons	Out/Indoor
66-71 GHz	No use known, but allocated to GNSS, ISS	Globally available. Wide bandwidth; multiple operators potential. Few sharing challenges. Harmonization potential	Future use for inter-satellite links arise	Outdoor/ Indoor
45.4-48.9 GHz	Radio Amateur Service and PMSE	45.5-47 GHz globally available. Wide bandwidth; multiple operators potential. Harmonization potential.	There are exclusive civil sub-bands which must be avoided. In Japan and China, the whole band may is not supported	Indoor
40.5-43.5 GHz	Mobile allocation is secondary. In Europe Fixed Service, but low use. In USA Fixed Satellite System. In Japan PMSE	Wide bandwidth; could support multiple operators. Collective use would be appropriate.	Global use. In Europe, the lower 2GHz has only a secondary mobile allocation, nowadays opened to fixed links. In USA and Japan there is not mobile allocation in the upper 1 GHz	Indoor
71-76 and 81-86 GHz	Point-to-point fixed links globally	Wide bandwidth. Good harmonization potential. Potential to use via extensions to light licensing	Global use. Commonly used for backhaul. Sharing may decrease reliability, unless self-backhauling is implemented	Outdoor
57-66 GHz	59-64 common global wideband data sub-band	Wide bandwidth. Good harmonization potential.	Global use. Currently allocated for wideband data, then its use could stop the scope for innovation by competing with WiGig	Outdoor/ Indoor
Below 6 GHz	Mobile allocations exist but saturated.	Good propagation properties; low path losses	Global intensive use. It is already saturated. Little bandwidth available.	Outdoor
28 GHz	Fixed Satellite and fixed links	High interest from the USA, Japan and Korea. Less path losses	Global use. Coexistence between service is still unknown.	Indoor
Above 100 GHz	Passive bands and Radio Astronomy Service (RAS)	Potential use to support backhaul	Global use. Range limited by atmospherics. Must respect the RAS	Outdoor

Table 1. Suitable frequency bands for the 5G standard

2.4 Transmission Standards

Previous sections speak about industry agreement in terms of architecture and technology, or possible interesting frequency bands for 5G network. Moreover, different microwave photonic techniques are described in the following sections. However, they are all proposals or recommendation. It is important to point out what is already standardized by the sector.

In [20], ITU-R defines the framework and overall objectives of the future development of International Mobile Telecommunications (IMT) for 2020 and beyond (IMT-2020). The objective of the recommendation is to determine the foundations for IMT-2020 by analyzing the growth, technological and application trends, as well as, potential user and spectrum implications.

IMT-2020 must support emerging new use cases. They are useful to resolve which will be the minimum requirements. On that basis, some of the most important trends will be the support of very low latency and high reliability human-centric communication (instantaneous connectivity), very low latency and high reliability machine-centric communication (M2M communication), high user density (satisfactory end-user experience in crowded events), high mobility at high mobility; enhanced multimedia services (media delivery with higher data rates); Internet of Things (connected devices growth); convergence of applications; and ultra-accurate positioning applications.

Many of these applications are derived from the future IMT traffic growth. Report ITU-R M.2370 estimates an increase in the range of 10-100 times from 2020 to 2030. The recommendation M.2083-0 also provides the technology trends mentioned in section 2.2. Moreover, it is pointed out the need to consider higher frequency ranges (between 6 and 100 GHz) what has led to the different studies on technical feasibility as the referred in section 2.3. During the World Radiocommunication Conference 2015 (WRC-15) several aspects related to the radio spectrum resources. In Resolution 238 (WRC-15) [21] ITU-R invited to complete in time for WRC-19 compatibility studies for an amount of frequency bands in the frequency range between 24.25 GHz and 86 GHz.

ITU-R list three main usage scenarios for IMT-2020: enhanced mobile broadband, ultra-massive machine type communications and reliable and low latency communications. The first one is linked to the increasing demand for mobile broadband together with new application areas and requirements. About massive machine type communications, future is envisioned as a world completely connected through a number of smart devices (Internet of Things). Lastly, ultra-reliable and low latency communications such as remote medical surgery should be supported.

Minimum technical requirements for IMT-2020 could be achieved with current IMT through enhancements, new components, technology and functionalities. Besides, services should be available anywhere, anytime. Thus, interworking between IMT-2020 and existing IMT, and between other radio systems is indispensable.

Recently, ITU-R has released a new report with the minimum requirements related to technical performance for IMT-2020 radio interfaces [22]. In Table 2 these requirements are reflected.

ATTRIBUTE		REQUIREMENTS	REMARKS
PEAK DATA RATE		DL: 20 Gbit/s	eMBB usage scenario
		UL: 10 Gbit/s	
PEAK SPECTRAL EFFICIENCY		DL: 30 bit/s/Hz	eMBB usage scenario. Defined assuming 8 and 4 spatial streams in DL and UL respectively
		UL: 15 bit/s/Hz	
USER EXPERIENCED		DL: 100 Mbit/s	eMBB usage scenario. Target values in the dense urban

DATA RATE	UL: 50 Mbit/s	environment.
5TH PERCENTILE USER SPECTRAL EFFICIENCY (BIT/S/HZ)	<u>Indoor hotspot – eMBB:</u> DL: 0.3 UL: 0.21 <u>Dense Urban – eMBB:</u> DL: 0.225 UL: 0.15 <u>Rural – eMBB:</u> DL: 0.12 UL: 0.045	eMBB usage scenario. The performance requirement for Rural – eMBB is not applicable in case of low mobility large cell.
AVERAGE SPECTRAL EFFICIENCY (BIT/S/HZ/TRxP)	<u>Indoor hotspot – eMBB:</u> DL: 9 UL: 6.75 <u>Dense Urban – eMBB:</u> DL: 7.8 UL: 5.4 <u>Rural – eMBB:</u> DL: 3.3 UL: 1.6	eMBB usage scenario. The performance requirement for Rural – eMBB is applicable in case of low mobility large cell.
AREA TRAFFIC CAPACITY	DL: 10 Mbit/s/m ²	eMBB usage scenario. Indoor Hotspot eMBB test environment
LATENCY	<u>User Plane:</u> eMBB → 4 ms URLLC → 1 ms <u>Control Plane:</u> eMBB and URLLC → 20 ms	eMBB and URLLC usage scenario. In user plane latency unloaded conditions for small IP packets in DL and UL is assumed
CONNECTION DENSITY	1.000.000 devices per km ²	mMTC usage scenario
ENERGY EFFICIENCY	Efficient data transmission in a loaded case. Low energy consumption when there is no data.	eMBB usage scenario
RELIABILITY	1-10 ⁻⁵ success probability of transmitting a layer 2 PDU of 32 bytes within 1ms in channel quality of coverage edge for the Urban Macro-URLLC test environment	URLLC usage scenario. Small application data assumed
MOBILITY	<u>Indoor hotspot – eMBB:</u> Stationary and Pedestrian <u>Dense Urban – eMBB:</u> Stationary, Pedestrian and Vehicular (up to 30 km/h) <u>Rural – eMBB:</u> Pedestrian, Vehicular and High speed vehicular	Stationary: 0 km/h Pedestrian: 0-10 km/h Vehicular: 10-120 km/h High speed vehicular: 120-500 km/h
MOBILITY INTERRUPTION TIME	0 ms	eMBB and URLLC usage scenario.
BANDWIDTH	100 MHz	RIT/SRIT shall support up to 1 GHz in frequencies above 6 GHz

Table 2. Minimum Requirements related to technical performance for IMT-2020 radio interface(s)

Until 2020 it is not expected to have the standard defined. To meet this objective, and in order to planning the development this timeline is considered:

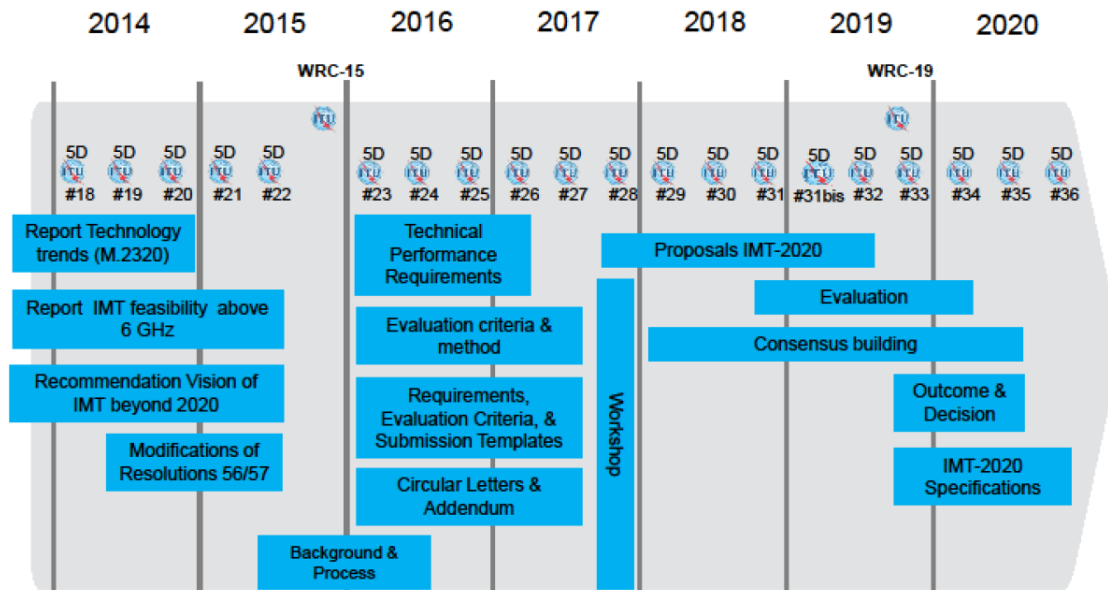


Figure 5. Timeline for the development of IMT-2020

Chapter 3. The role of microwave photonics

Once the 5G standard is introduced, it is necessary to get introduced in the role that microwave photonics can play inside the standard. Microwave photonics is a mature multidisciplinary engineering field that attempts to utilize the properties of photonic technologies to improve the performance of microwave/wireless systems [16]. The properties of the field make it a perfect candidate to help in the implementation of the technology.

There are many possibilities under study to be employed inside the 5G network. Throughout this chapter distinct roles will be introduced.

The chapter has been divided into the next sections:

- Section 3.1 introduces the Radio-over-Fiber (RoF) Transmission
- Section 3.2 introduces two Indoor Frequency Up-conversion RoF Link Schemes
- Section 3.3 introduces the RF Signal Photonic Generation
- Section 3.4 introduces the Optical Conformation
- Section 3.5 introduces the Filtering

3.1 Radio-over-Fiber (RoF) Transmission

Inside the indoor architecture shown in section 2.1, microwave photonics plays a significant role. The small-cell wireless system described is also referred as Distributed Antenna System (DAS). In the scheme, fiber is used to distribute the cellular signals, captured on the roof of a building or received through optic-fiber, to each floor. The transport scheme employed is Radio-over-Fiber (RoF).

A RoF link consists of a directly or externally modulated laser, where one or more analog electrical signal placed at different microwave frequencies is imposed to an optical carrier, and a detector after the optical fiber link, where the microwave signal is recovered from the optical carrier[23]. Its principal features are the capability to easily support multiple wideband signals (multiple operators and multiple services), centralized frequency channel management, central office (CO) equipment sharing and the simpler antenna remote units (ARUs) as no frequency conversion is required[16].

3.1.1 Figures of Merit and RoF Link Limitations

To evaluate the performance of these links a set of figures of merit (FOM) are typically considered: the RF link gain (G_{RF}), the noise figure (NF) and the spurious free dynamic range (SFDR). G_{RF} in RoF links is defined as the ratio of the RF power delivered to a matched load at the photodetector output, $P_{RF|OUT}$, to the available RF power at the input, $P_{RF|IN}$, delivered to the modulation device, both at the modulating angular frequency Ω [24]:

$$G_{RF} = P_{RF|OUT}(\Omega) / P_{RF|IN}(\Omega).$$

The microwave signal suffers a degradation as a result of the existing noise sources. To evaluate this deterioration noise figure is adopted.

$$NF = N_{TOT} / (G_{RF} N_{IN})$$

, where N_{TOT} and N_{IN} are, respectively, the total output and input noise spectral densities. The SFDR is used to characterize the linearity and noise characteristics of microwave devices, analogue-to-digital converters and optical devices such as laser diodes and external modulators. This FOM is defined as the carrier-to-noise ratio when the noise floor in the signal bandwidth equals to the power of a given order intermodulation product. The prominent problem in RoF links is the third-order (IMD3) intermodulation distortion. This force to maintain a small nonlinearity system to achieve a high SFDR. The SFDR for IMD3 can be computed from $SFDR_3 = (OIP3/N_{TOT})^{2/3}$, where OIP3 is the linearly extrapolated input power at which the fundamental and the IMD3 output power would be equal.

From the view of the FOM, nowadays still exist some problems in this kind of links. In [23], three challenges are identified.

- Firstly, **high-linearity conversion and control between the lightwave and microwave**. The linear conversion between light- and microwaves determines the upper limit of the dynamic range of the RoF link. Both harmonics and IMD may be induced by the nonlinear transfer function of the MZM. Besides, the fiber link suffers from environment perturbations which degrade the phase stability to be delivered.

Two methods for high-dynamic-range RoF links and highly stable RF delivery links are discussed. To overcome the linearity conversion the main optical contributors of the IMD3 are identified and suppressed directly in the optical domain through a special phase shift introduced to the optical carrier band (OCB) processor. It shows an increase in fundamental-to-IMD3 from 30 dB to 68 dB, and from 99.6 to 114.3 dB·Hz^{2/3} in the SFDR. To realize the RF phase controlling a phase compensation scheme based on an active compensation loop is proposed. The loop consists of a large-tunable-range optical delay and a regular phase discriminator. It takes advantage of the large accumulated link dispersion resulting in a “ λ -dispersion” tunable delay. Broadband stable RF signal delivery with a large compensation range is achieved.

- Secondly, **fine processing and handling of broadband microwave signals**. The challenge is to combine the broadband processing capability of photonics and the fine-resolutions processing capability of electronics. An optical frequency comb (OFC) bridges the gap between the broadband optical and the precise microwave in a single step. Two methods to real-time, high-resolution monitoring of the RF spectrum and a scheme for multiband microwave frequency conversion are introduced.

- Thirdly, **efficient utilization and dynamic management of the resources in the DAS**. In some DAS applications, a single set of base-station facilities in the center unit is connected to multiple antenna units (RAUs) to extend the indoor coverage of one base station and to share the bandwidth resource. In 5G, this application will be employed to meet the high-rates and low latency requirements with small-cells covering indoor spaces. In the paper, the performance of the existing IEEE 802.11 MAC protocols, point coordination function (PCF) and distributed coordination function (DCF), in simulcast WLAN RoF DASs is investigated. The adaptive PCF is a promising mechanism in terms of the overall throughput and fairness among RAUs.

3.1.2 RoF role in Virtualized RAN

In [15], the cloud radio access system technology for the virtualized RAN (vRAN) proposed for the 5G architecture is introduced. The main idea is to realize the mobile backhaul/fronthaul of small-cells in outdoor environment via RoF as in the indoor environment. C-RAN simplifies the ARUs by shifting MAC layer functions and baseband signal processing to the central office (CO) or Baseband units (BBU) and the small-cells backhaul is accomplished transmitting digital I/Q samples. This requires very high throughput and total capacity of backhaul networks. Moreover, the separation between MAC and PHY layers require an intensive control of latency and jitter in the CPRI.

In the vRAN case the ARU's function is simpler by shifting DAC/ADC and RF frontend functions to the BBU. In ARUs only remain O/E-E/O conversion and RF antennas. RF signals are generated at BBU and transmitted to ARUs through fiber-optic backhaul by means of RoF. It allows more cost-effective and scalable small-cell backhaul; infrastructure sharing by multiple operators, multiple services and multiple wireless techniques (e.g. MIMO) while maintaining independent configurability through the centralized network management.

3.2 Indoor Frequency Up-Conversion RoF Link

Indoor architecture described in section 2.1 is composed by a central unit (HCC), responsible for central control and management unit, and the RN and the RAPs. The gateway functions are a key to well address all network functions. There are three main categories of signal processing to be dealt with in the gateway: (1) converting baseband digital signals in Optical Access Networks (OAN) to/from indoor RF signals, (2) converting IF data signals in OAN to/from indoor RF signals and (3) transparent handovers of RF data signals from OAN to/from indoor network without conversion.

To deal with the conversion needed in signal processing (1) and (2) three functions are required in the gateway. First is the baseband DSP, dealt with signal modulation and other DSP functions. Second is the frequency up-conversion, which up-converts baseband data onto mm-wave carrier frequency. Third is indoor exchange (IE) functions, which allow data switching and routing inside the indoor fiber networks. In [25] two frequency up-conversion techniques are proposed to achieve flexible reach data delivery, convenient frequency up-conversion and versatile indoor exchange.

In all-optical remote up-conversion (RUC) technique, both optical baseband data and optical mm-wave frequency are sent to the gateway (GW) with up-conversion realized in a remote site. The scheme is shown in Figure 6. Baseband (BB) data is modulated on a wavelength in the CO and then delivered to a RN. In the GW, the wavelength is split into two paths, one for the downlink and other for the reflected uplink. Optical signals are assigned to

different flats/rooms in a dynamic way. Time division multiplexing (TDM) is employed, so the BB wavelength will be routed to different destinations in different time frames.

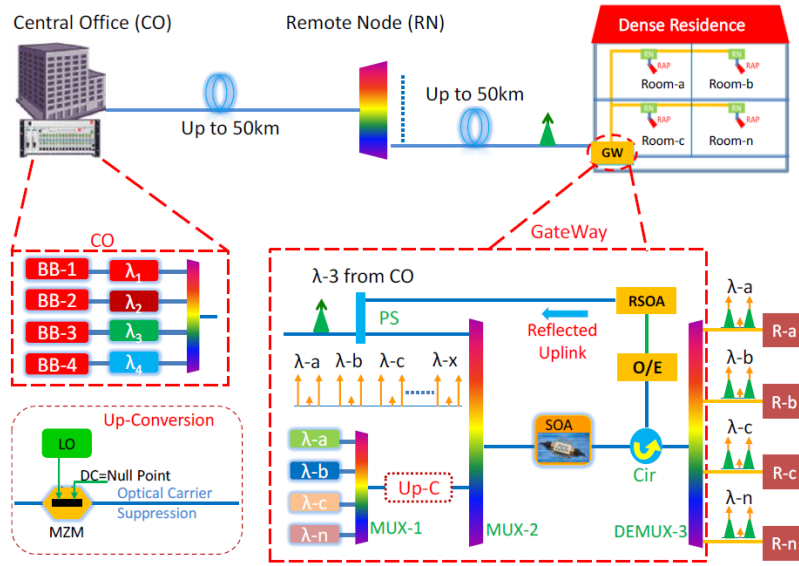


Figure 6. Operation principle of all-optical remote up-conversion and indoor exchange

The dynamic allocation is realized by turning on specified wavelengths. They are multiplexed via an optical multiplexer (MUX-1) and modulated using a local MZM biased at its null point with a 30 GHz local oscillator (LO). The blank 60 GHz optical mm-wave generated at determined wavelengths. After being multiplexed (MUX-2) with the BB wavelength, the output is fed into a SOA. Cross Gain Modulation (XGM) process in the SOA modulates the BB data to the 60 GHz mm-waves. The result is separated by a de-multiplexer (DEMUX) and distributed to different apartments/rooms. The optical routing is realized by switching on one specific local wavelength while switching off the others. The IE functionality is colorless for the CO.

For the uplink to the CO the data from each apartment/room are detected and then modulated via a reflective SOA. The downlink wavelength injected to RSOA is amplified and reflected out of RSOA with data modulation. Therefore, the uplink wavelength is reused from downlink wavelength with colorless operation.

Experimental results show that 5 Gb/s OOK data carried by a 60 GHz hybrid fiber wireless channel over 102 km SMF is successfully delivered with a power penalty less than 1.1 dB. Routing and optical multi-casting are demonstrated as well.

In free-running laser-based optical heterodyne technique (OH) the baseband data is modulated on one wavelength and the other wavelength is used for optical beating to up-convert the baseband data. No electrical local oscillator is involved. The diagram of the proposed system is shown in Figure 7.

The baseband data of users are delivered from the CO to the GW of a densely-populated region. At the GW are located all the functions except for frequency up-conversion. After baseband processing, the processed signals are modulated onto different wavelengths, assigned for the respective destinations. Inside the HCC, a set of arrived wavelengths (λ -3, λ -4) pass through an optical circulator (Cir1) and coupled with the optical local oscillator signals (λ -3b, λ -4b) via an optical coupler. The optical local oscillator signals are generated with two tunable lasers. The coupled optical signals pairs travel toward the second circulator (Cir2). Due to the fiber transmission induced polarization rotation, crosstalk occurs (OH process). The optical signals are delivered to different rooms using a wavelength de-multiplexer (DEMUX).

This architecture is scalable and all wavelengths can be used since there are dedicated optical fiber connections from each HCC to the GW. By tuning the wavelength of λ -3b and λ -

4b, the frequency of the generated mm-wave can be flexibly adjusted to satisfy the dynamic spectral allocations.

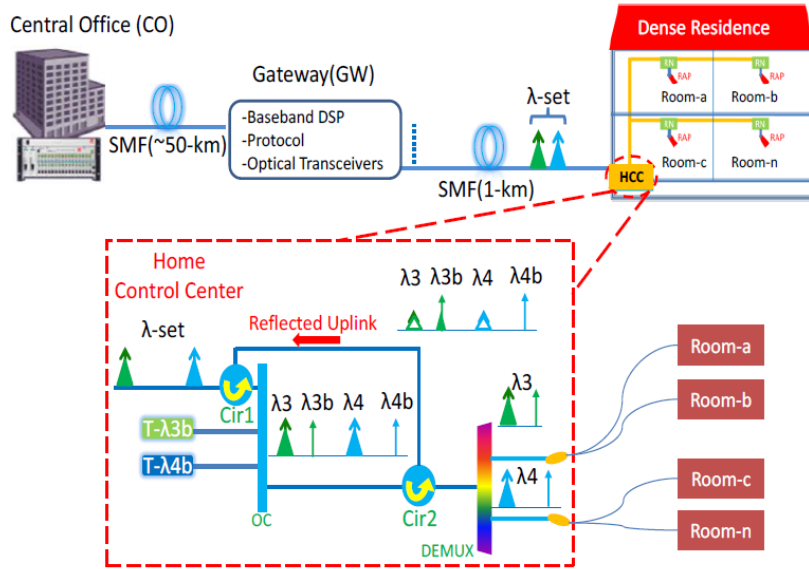


Figure 7. Principle of the hybrid fibre wireless indoor network based on the optical heterodyne techniques

Experimental results demonstrate that the system is able to deliver a 61.3 Gb/s MIMO-OFDM signal over 1 km SMF-28 fiber and 1 m wireless link at 40 GHz. The proposed system is very attractive for 5G high-speed wireless indoor scenarios.

Moreover, in [25] a simple control signalling delivery for the GW of indoor networks is studied. The control signalling is important for the realization of network functions (e.g. adapt RN) and only occupies a limited bandwidth. The proposed architecture of reconfigurable WDM OFDM access networks consist of a ring-tree topology. Single-fibre wavelength division trees are connected to the WDM fibre ring at RNs. Each RN has to drop and add signals at two independent wavelengths. All signals can be launched into the ring fibre in both directions. Optical network units (ONUs) and RNs are connected via a power splitting distributive PON. Each PON shares an optical channel on a TDM and a FDM basis.

The low frequency control channel insertion and detection (LFID) scheme is utilized in the architecture described. The OOK modulated low speed signalling is added to the OFDM signal, preferably in the digital domain. After combining, the combined digital waveform is converted to an analog signal through a DAC and then modulated on the optical carrier via a MZM constructing a directly detected, low cost and no frequency guard interval optical OFDM transmitter. After the transmission over the fibre ring, the RN will receive the optical signal after an asymmetric optical splitter. A low speed photodiode followed by an electrical low-pass filter is employed to detect the combined signal and to remove the OFDM signal. Then the signalling (OOK signal) can be retrieved using low speed logical circuit and the user data (OFDM) can be also well retrieved in the ONU, even without any electrical high-band pass filter.

3.3 RF Signal Photonic Generation

In previous section two schemes for frequency up-conversion are presented. To generate high-frequency and wide-band microwave and millimeter-wave signals, different photonic generation techniques are being considered due to their advantages over electrical techniques. These techniques include the methods based on external phase or intensity modulators, optical injection locking (OIL), optical phase-locking loop (OPLL) and optical injection phase-locked loop (OIPLL). However, at high frequencies all these methods, except the first one, are complicated to implement and/or expensive. Optical generation methods based on external

modulation are of great interest thanks to the wide frequency range and excellent stability of the system. Since the most interesting mm-Wave frequencies for 5G indoor are in the range from 40 to 71 GHz, it would be relevant to achieve a tunable generation system able to produce mm-wave signals in this range.

Four different generation techniques based on external modulation are introduced.

3.3.1 Triangular-shaped microwave pulses generation based on SBS

In [26], a triangular-shaped microwave pulse generator based on the external modulation of a CW light wave is proposed. Triangular waveform has only odd-order harmonics. Therefore, a MZM biased at the minimum-transmission-point (MITP) is used to generate only odd-order optical sidebands.

The schematic diagram of the generator is shown in Figure 8. It consists of a laser diode (LD) whose light wave is divided into two parts by an optical coupler (OC). A frequency shifter raises the frequency of one part to operate as the pump of SBS. The frequency shift can be realized by using carrier-suppressed double sideband modulation. The other part is modulated in the MZM by a RF signal. The result is a light wave with only odd-order harmonics. The SBS pump light and the modulated light wave introduce themselves in a highly nonlinear fiber (HNLF) in opposite directions. Then the processing of the modulated signal using SBS is performed. An OBPF filter the unwanted optical sidebands leaving only the carrier and the 1st and 3rd order sidebands. The 2nd order harmonic can be neglected after the conversion in a PD.

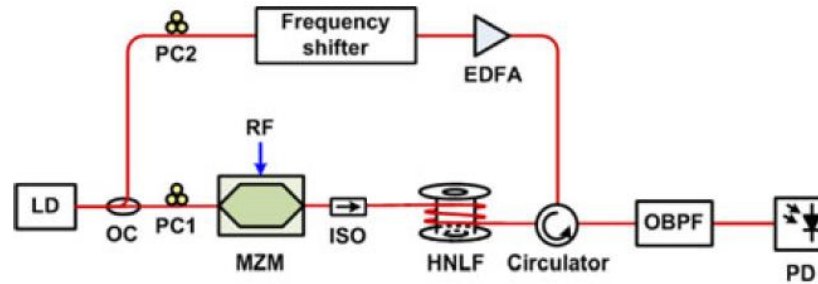


Figure 8. Schematic diagram of the generation of triangular-shaped microwave pulses

Although triangular waveform consists of a large variety of odd-order harmonics, high order harmonics with fast roll-off factor have so insignificant impact that two odd-order harmonics are enough. Moreover, the influence of the 2nd order harmonic decreases with the power of the pump light and the length of the fiber. Nevertheless, an appropriate SBS gain should be investigated as high-power EDFA and long fiber reduce the waveform quality.

If the optical carrier deviates from the peak of the SBS gain spectrum nonlinear phase shift will induce waveform distortion. The tunability of the system is achieved through the variation of the RF signal frequency applied to the MZM. Hence, it results a stable generation system with fine accuracy in parameter control.

3.3.2 Optical microwave generator based on SBS with fine tunability

In [27], a novel scheme based on the same principles is proposed. The system revolved around a MZM biased at MITP to realize CS-DSB modulation and a frequency shifter based on SBS also (Figure 9).

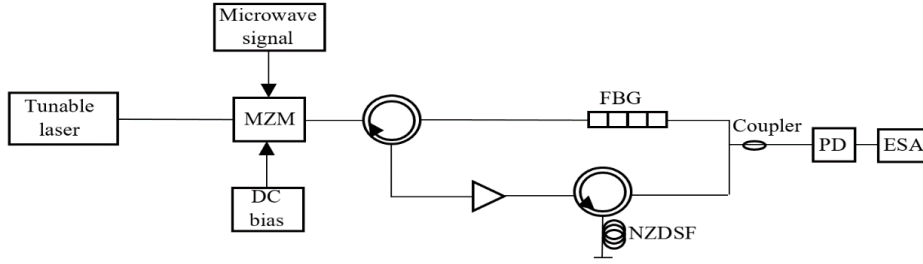


Figure 9. Schematic diagram of the proposed microwave generator

In this case, the light wave (f_0) is first modulated by the RF signal (f_m) in the MZM and then, through a circulator and a Fiber Bragg Grating (FBG) the lower sideband is reflected to act as a pump wave that stimulate the SBS process. In the lower branch is amplified by an EDFA and then it gets in a frequency shift module realized inside a None Zero Dispersion Shifted Fiber (NZDSF) with the SBS effect. The frequency difference between the shifted lower sideband and the upper sideband is enlarged with a SBS frequency shift. Once the two components are coupled out and beat in a photo detector (PD), a microwave signal with a frequency equal to the frequency difference of the two sidebands is detected: $f_{RF} = 2f_m + \nu_B$.

Experimental studies achieve a SNR ranging from 20 to 30 dB. This variation is caused by the changing response of the MZM used and the responsibility of the PD with the modulation frequency and the bandwidth of the input signal, respectively. Moreover, the reflective spectrum of the FBG used is not flat so, the intensity of the lower sideband reflected by the FBG varies as the modulation frequency is changed.

The system can be tuned by changing the frequency of the RF signal applied to the MZM. The experimental results show that microwaves in the range from 14,67 GHz to 30,67 GHz by tuning the frequency of the RF signal from 2 GHz to 10 GHz can be achieved with a SNR higher than 20 dB.

3.3.3 Tunable DC-60 GHz RF generation via a dual-loop OEO based on SBS

Optoelectronic oscillator (OEO) can generate millimeter wave signals with ultra-high frequency and high spectral purity. Commercial electrical band-pass filters are not able to work with a broad frequency band, so the tuning range of the OEO is limited. However, this limitation is overcome with the arrival of microwave photonic filters (MPFs), and OEOs are being designed as a tool in millimeter-waves generation. In [28], a tunable OEO based on SBS, in which RF signals from dc to 60 GHz can be generated, is defined.

Narrow-band MPF is synthesized by means of combining phase modulation and selective sideband amplification by SBS, and a dual-loop configuration is used to eliminate the frequency drifting and mode hopping.

The system architecture is shown in Figure 10. In this case, two lasers configuration is adopted to generate the pump (ν_p) and the signal (ν_0) wave. Both waves are injected into HNLF but in opposite directions. The resulting wave of the SBS process is a backscattered Stokes wave with a frequency downshift ν_B relative to the pump wave. The light wave flow through two SMF after a 3 Db optical coupler (OC) and after beating two photodiodes (PD) they are coupled together and amplified by a low noise amplification (LNA) and a power amplifier (PA). This signal is fed back to drive the PM to form a closed loop. The beat between signal wave and amplified 1st sideband will be the final oscillation mode.

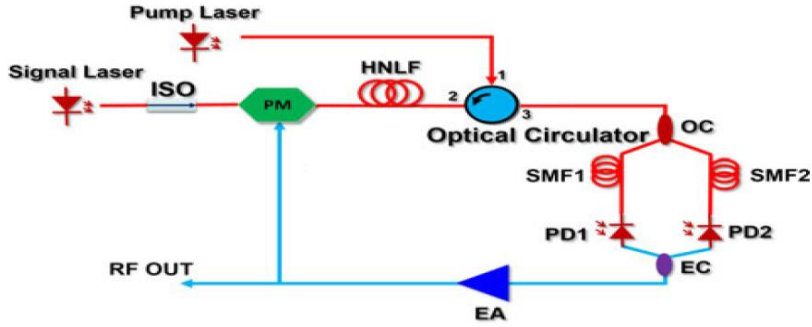


Figure 10. Schematic diagram of the proposed dual-loop OEO based on SBS

The oscillation frequency adjusts to: $v_{osc} = |v_0 - v_p + v_B|$. Therefore, by tuning the wavelength of pump laser, the oscillation frequency changes. The frequency tunability range is determined by the frequency response of the optoelectronic components in OEO's loop. Besides, the tuning step is limited by the wavelength tuning step of the pump laser.

3.3.4 39-GHz millimeter-wave carrier generation in dual-mode colorless laser diode

In [29], a 39 GHz mm-wave carrier generator is developed. The system is supported by a null biased MZM for CCS-DSB modulation and dual-mode injection-locking of a directly encoded colorless laser diode.

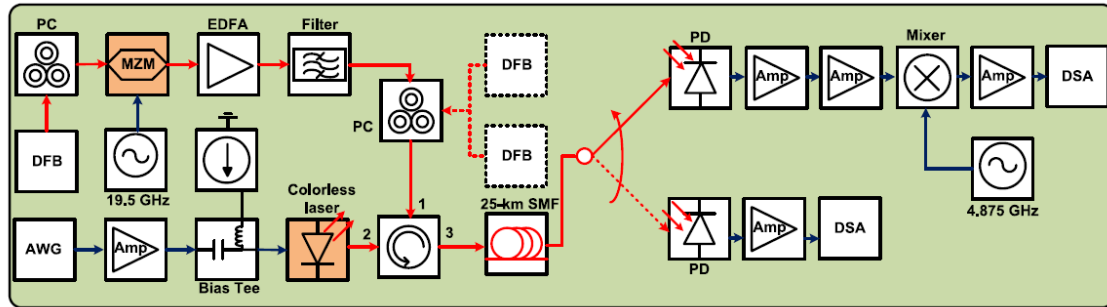


Figure 11. Experimental setup of CCS-DSB or dual-DFBLDs injection-locked slave colourless laser diode

The schematic diagram proposed is shown in Figure 11. The CCS-DSB master of the injection-locking is generated by modulating a CW light from a DFB laser diode (DFBLD) with a null-point biased MZM. After amplifying the modulated signal and filtering its ASE noise with an optical bandpass filter, the final dual-mode master is seeded into the slave (colorless laser diode) through an optical circulator. The electrical data to be delivered is pre-amplified and its DC-level is offset by a bias tee for directly modulating the colorless laser diode. After a 25-km SMF transmission the data is received by a photodetector (PD), converted back to electrical data and amplified by an electrical amplifier. If a localized wireless mm-wave access link is the aim of the carrier generated a high-speed PD is employed with two high gain mm-wave amplifiers. Then the mm-wave carrier is frequency down-converted to the baseband with a 4.875 GHz local oscillation frequency.

The performance of the proposed system is analyzed if CCA-DSB modulation or dual-DFBLDs configuration is employed. As the central carrier of the master and the side-modes of the injection-locked colorless laser diode can be suppressed in CCA-DSB (central carrier added – DSB) because they will not be resonantly amplified, CCS-DSB represents a better option.

After the 25-km SMF, the residual central carrier and the FWM modes deteriorate the transmission performance in the CCS-DSB case. However, the photonic mixed mm-wave carrier in dual-DFBLDs is unstable in frequency domain because of the wavelength instability of 2 DFBLDs. Consequently, the CCS-DSB modulation is the most appropriate.

3.4 Optical Conformation

Massive MIMO is supposed to be a key technology in 5G performance. At mm-wave, the system is less interference limited, however the higher path loss requires coverage enhancing solutions. With regards to compensate the path loss, employing beamforming capable directional antennas is the industry proposal.

Beamforming is a technique to focus and steer the radio signal beam (or signal power) to the desired directions. Instead of transmitting in all directions, antennas confine signal power in a particular direction of interest. This is truly important in the indoor scenario and architecture described, as it helps to provide the desired wider area coverage by dynamically steering the beam to the user devices inside the cell coverage area. Moreover, it can reduce the energy consumption in the transmitter as it requires less transmission power to achieve same amount of signal power at receiver.

By focussing in certain directions, the interferences are limited to small fractions of the entire space around a transmitter improving the radio environment. It will also be useful at lower frequencies to extend coverage and to provide higher data rates in sparse deployments for example.

Because of their fast steering and compactness, phased array antennas (PAAs) seems to be the most attractive beamsteering method at the mm-wave band. The technique is based on the control of the phases/amplitudes of the radio signals radiated by the antenna elements to induce constructive combination at desired directions and destructive ones at other directions.

Given N elements of a PAA, the antenna gain and SNR improvement can be achieved by a factor of N . The PAA elements should be separated at least half the wavelength of the radio signal. Therefore, the small wavelength at mmWave frequencies implies that the antenna elements will be closely spaced, facilitating the compactness of a large-size PAA.

Traditionally, beamforming is realized in electronic circuits. Samsung has recently proposed and demonstrated a mm-wave communication empowered by beam steering based on electronic devices[30]. The use of phase shifters limits the operational bandwidth of a conventional PAA. True Time Delay (TTD) is the basis for broadband beam steering but electronic integrated circuits suffer from high loss at high frequencies. The emerging technique is TTD beamforming by means of optical circuits (OTTD) to benefit from their low loss and broad bandwidth.

The indoor architecture envisioned in section 2.1 makes beamforming different from the traditional beamforming because of the remote baseband processing. The RoF benefits from OTTD since no additional E/O-O/E conversion is necessary. Besides, it keeps the RAPs simple, a fundamental feature in RoF architectures. In the architecture description is mentioned that the HCC must remotely control, among other aspects, beam steering. OTTD does it by changing the optical wavelengths, and it avoids extra control signal requiring strict synchronization.

In [31], a 38 GHz beam steered millimeter-wave system based on OTTD and two architectures for such beam-steering are proposed. A remotely tunable integrated optical tunable delay line (OTDL) based on an arrayed waveguide grating feedback loop (AWG-loop) is employed. Figure 12 illustrates the proposed system.

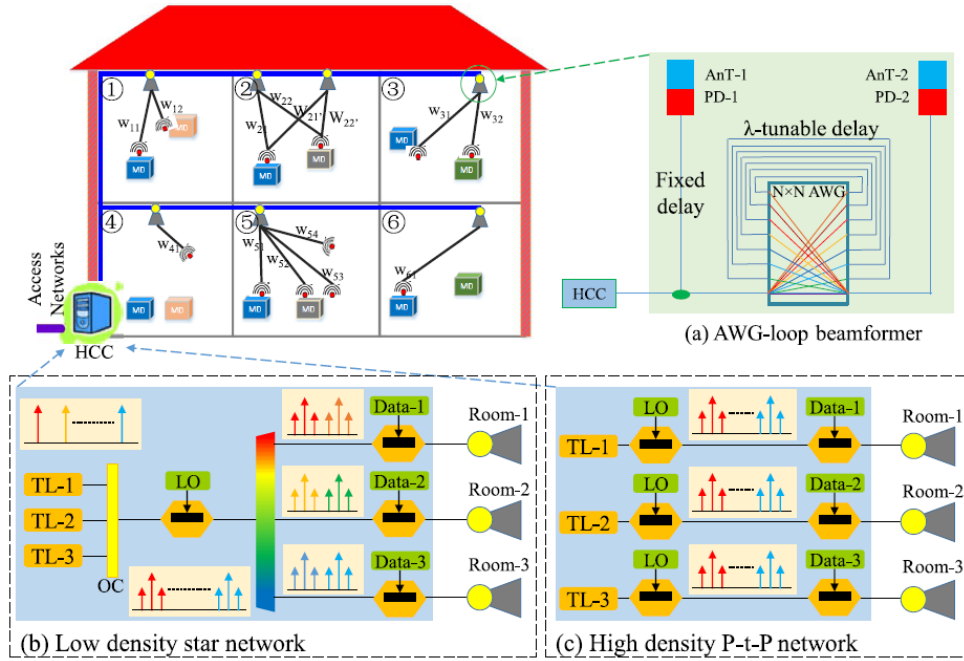


Figure 12. 38GHz wave beam steered fiber system

The AWG-loop is composed of an N-by-N spectral cyclic AWG. This AWG is employed as both the wavelength MUX and de-MUX. N-1 pairs of inputs and outputs are connected in a symmetric configuration for re-circulating operations. The optical signal is split into two paths: one goes directly to the first output and the other goes to the AWG-loop and the second output. When RoF signal impinge on the AWG it introduces delays which depends on the wavelength of the RoF signal. The RoF signals choose a path with specific delay, which depends on the wavelength of the signal. The delay depends on the dispersion coefficient of fiber, the length of the path traversed and the free spectral range of the AWG. Hence, the delay of the output can be selected by tuning the wavelength of the signal. To compensate the travel time of the AWG-loop a compensation optical delay line (CODL) is employed.

This AWG-loops are installed at the end of the network as remote access points. The wavelength tune is realized by the HCC. In the paper two network architectures for the HCC are shown. First, a low-density star network with low beam density, complexity and cost. On the other hand, a high-density point-to-point network with high beam density, but also more complexity and cost. Experimental results show that bit rates from 50Mb/s to 8 Gb/s per spatial channel are possible with the beam steering system proposed.

All in all, beam-forming in a RoF architecture, as the described, can be achieved by tuning the wavelength of the signal (HCC), and utilizing an AWG-loop and a compensation optical delay line to produce the desired delay and compensate the travel time (RAP).

3.5 Filtering

Inside the microwave photonic there is a variety of applications of paramount importance in the future 5G networks. One of the fields under research is the realization of filters through microwave photonic systems. This is known as microwave photonic filters. It consists of a photonic system designed with the goal of implementing the equivalent tasks to those of an ordinary microwave filter within a radio frequency (RF) system or link. The interest in MWP filters is due to the advantages inherent to photonics such as low loss, high bandwidth, immunity to electromagnetic interference, tunability and reconfigurability.

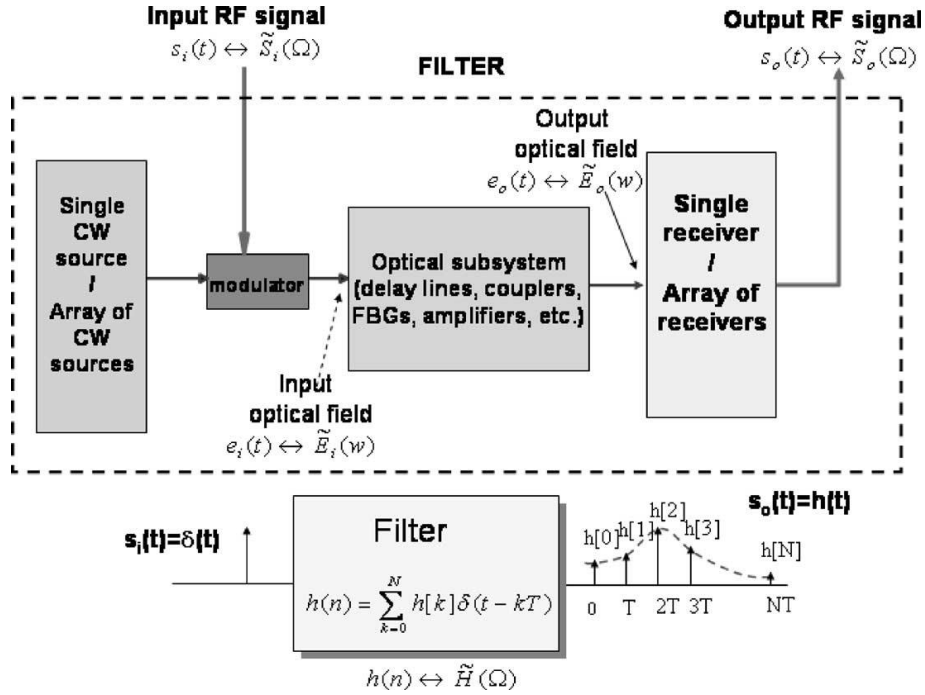


Figure 13. General reference layout of a microwave photonic filter

Figure 13 illustrates a general reference layout of a MWP filter. The RF to optical conversion is realized by directly (or externally) modulating a single continuous wave (CW) source or a CW source array. The input RF signal is carried by the optical carrier and the resulting signal is fed to a photonic circuit that samples the signal in the time domain, weights the samples and combines them using optical delay lines and other photonic elements [32]. The output optical field is optically RF converted. The lower part of Figure 13 shows an equivalent black-box representation of the aimed performance of the MWP filter. The only signal linearity is that relating the input and output optical fields to the optical subsystem by virtue of the linearity of Maxwell's equations. According to the number of samples N in the impulse response sequence, the filter can be classified as a finite impulse response (FIR) if $N < 8$ or an infinite impulse response if $N > 8$.

The transfer function is spectrally periodic with a period of $2\pi/T$ in angular frequency units or $1/T$ in frequency unit. Therefore, the spectrum is periodic. The period mentioned is known as the filter free spectral range (FSR).

In the paper two kinds of MWP filters and possible implementations are introduced. On the one hand, single-source microwave photonic filters are characterized by the use of only one optical source to feed the filter. The source output electric field is modulated by the RF input signal and the different filter samples are implemented by means of delayed and windowed replicas of the RF-modulated optical carrier. Two possible implementations of a FIR and an IIR SSMPF are shown. On the other hand, in multiple-source microwave photonic filters the RF input signal optically combines and modulates the output of an array of optical CW sources. The source array can be implemented through an array of independent lasers or by slicing the output of a broadband source by means of a periodic optical filter. Each source implements a filter sample that is selectively delayed by employing a dispersive line implemented either by a fiber coil or by a linearly chirped fiber Bragg grating (LCFBG). The dispersive delay element is chosen such that the differential group delay experienced by adjacent wavelengths of the source array is T .

However, MWP filters must still overcome potential limitations either in the optical and the electrical domain. Within the optical domain, it is found the spectral periodicity, which limits the bandwidth of the RF signal to be processed to a fraction of the FSR in order to avoid spectral overlapping; the positive coefficients, because it limits the range of transfer functions that can be implemented; fiber nonlinearities such as self-phase modulation (SPM), cross-phase

modulation (XPM), four-wave mixing (FWM), etc; polarization effects; limited spectral period; reconfigurability and tunability. In the electrical domain the total RF gain, the noise figure and the harmonic and intermodulation distortion are the limitations to overcome.

There is a wide range of applications inside 5G networks where MWP filters can be of interest. In the way to increase the capacity, RoF systems enable to centralize the RF signal processing functions in a shared location (headend) simplifying the remote antenna units (RAUs). The processing at the headend involves a prior frequency down-conversion, ADC, and baseband processing using a DSP. The down-conversion can be eliminated or divided into two steps if a MWP filters placed prior to optical detection.

Besides, they can help to suppression the noise and to mitigate the channel interference, very important in a high-density environment. Moreover, they can also be employed in the field of true-time delay beam steering of antenna arrays. The feeder network of an array of N antennas is essentially equivalent to an N-tap MWP tunable FIR filter where the basic filter delay T can be altered. The only difference is that each filter sample is detected by a different optical receiver that is placed before each antenna unit in the array.

Chapter 4. System Designs, Simulations and Results

As it has been shown, there are many applications for Microwave Photonics in 5G indoor environment. This work revolves around the generation of mm-wave signals through Microwave photonics techniques.

Four different techniques are presented, one of this is focused in generate Triangular-Shaped pulses instead of generating high-frequencies signals through lower-frequencies oscillators. All of them are based on the use of one Mach-Zehnder modulator to generate the mm-wave signal; and the Stimulated Brillouin Scattering (SBS) will play an important role in some of the techniques.

To simulate the systems and check their performance VPI photonics software has been chosen as the simulation platform software.

The chapter has been divided into the next sections:

- Section 4.1 describes the simulation platform software
- Section 4.2 explains a transmission scheme which does not make use of MWP techniques to transmit the information
- Section 4.3 shows an alternative design to transmit the information by employing MWP techniques
- Section 4.4 shows the simulation process of the optical microwave generator based on SBS with fine tunability introduced in section 3.3
- Section 4.5 shows the simulation process of the triangular-shaped microwave pulses generator introduced in section 3.3
- Section 4.6 introduces a proposed mm-wave generator based on two lasers with enhanced flexibility

4.1 Description of the Software

As already noted, VPI photonics is the simulation platform software on which the simulations realized are based.

VPI photonics is a professional simulation software which allows to end-to-end photonic design automation comprising design, analysis and optimization of components, systems and networks. It supports requirements of active/passive integrated photonics and fiber optics applications, optical transmission system and network applications, as well as cost-optimized equipment configuration.

VPI photonics requires the following minimum configuration:

- 1 GHz or faster 64-bit (x64) processor
- 2 GB RAM
- 2 GB of free hard disk space for software installation process, 1 GB additionally recommended for file storage
- XGA monitor with 1024x768 pixels minimum display resolution
- DirectX 9 graphics device with WDDM 1.0 or higher driver
- For GPU-assisted computations NVIDIA video adapter with compute capability greater than or equal to version 1.3 and double-precision support is required
- DVD-ROM drive
- Windows 7, Windows 8.1 or Windows 10 Enterprise

The system is based on the union of different modules which can represent components, converter units, analysers, etc. All the systems simulated in this thesis lean on three modules: Mach-Zehnder modulator, a DFB continuous-wave laser and a photodiode. These three modules remain unchanged in all the systems.

The Mach-Zehnder modulator module employed has the following parameters:

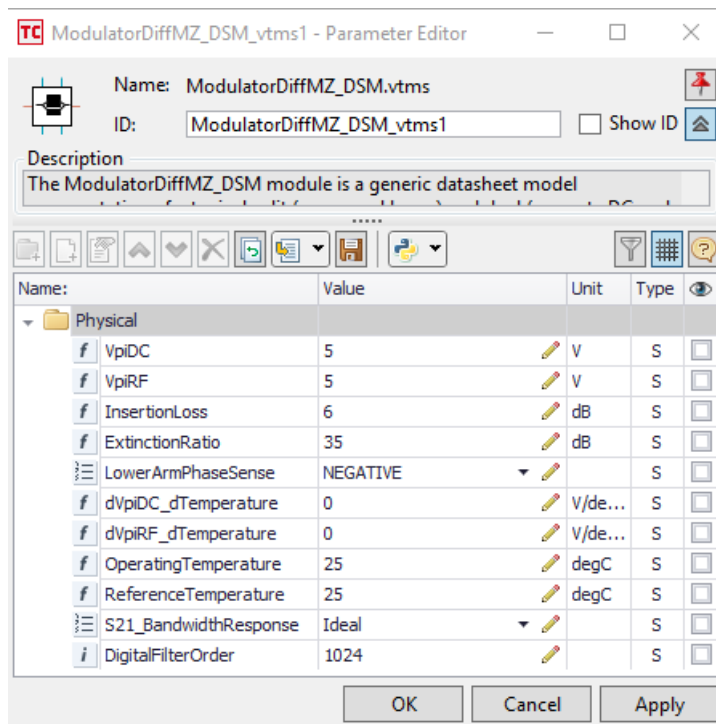


Figure 14. Parameters MZM module

With the previous characteristics, its normalized transfer function is as depicted in Figure 15.

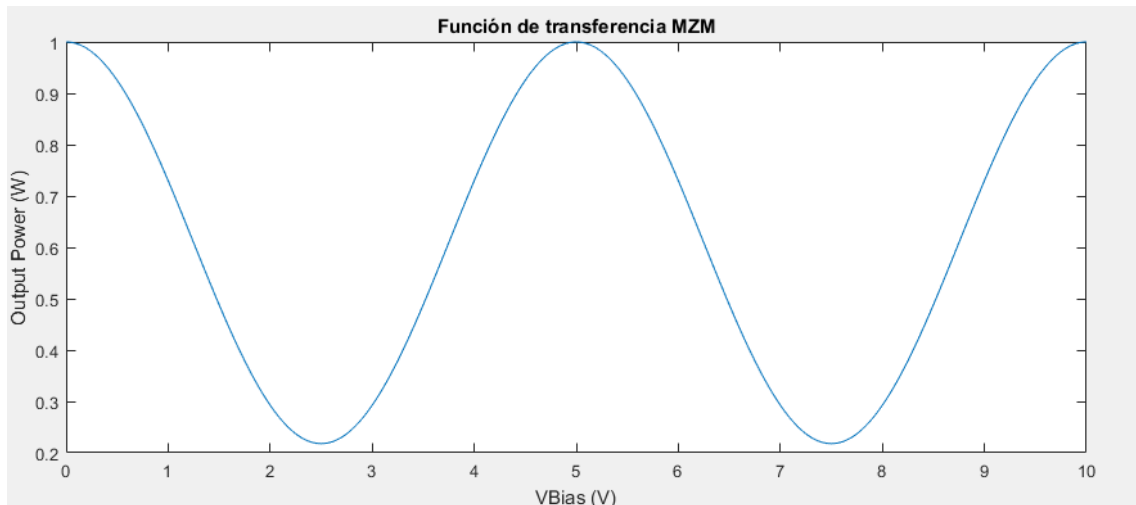


Figure 15. MZM transfer function

In this way, the minimum-transmission-point (MITP) or null-point is at 2.5 V and the quadrature-point at 3.75 V. These are the main biasing points employed, the first for double-sideband carrier suppressed modulation (mm-wave generation) and the second for data modulation.

On the other hand, the laser is a DFB continuous-wave laser centred in 193.1 THz, with an average power of 10 mW and 10 MHz of linewidth.

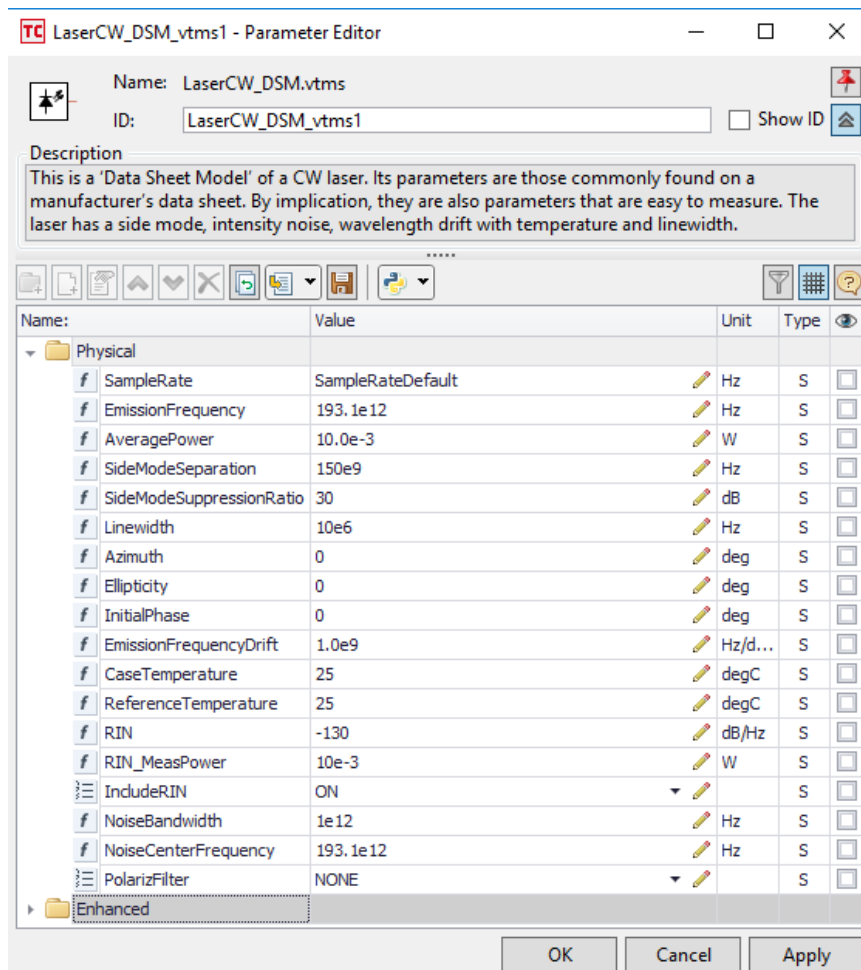


Figure 16. Laser parameters

Lastly, the receiver module employed is a basic model of PIN photodiode with a 1 A/W responsivity, $10.0e-12$ A/Hz thermal noise and without dark current.

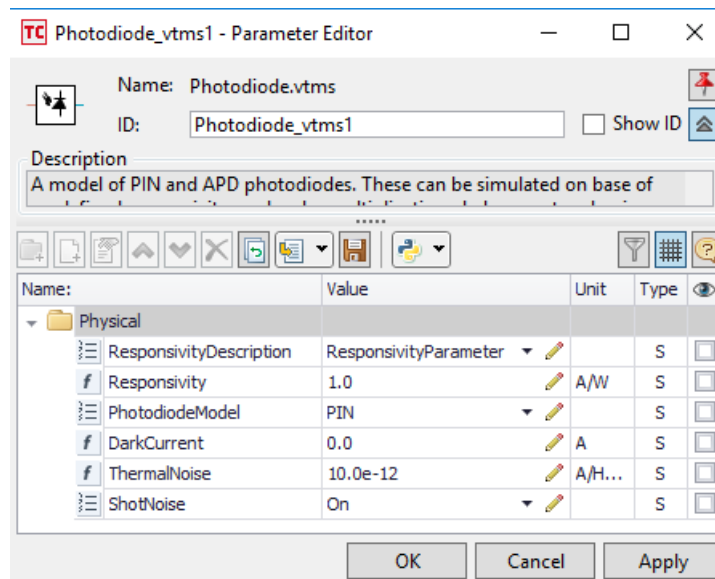


Figure 17. Photodiode parameters

Although the main issue is the RF signal photonic generation, data transmission is tested in the two first systems. To analyse their performance the bit error rate (BER) is measured. The module employed to do it is a BER estimator for OOK modulation (the data modulation employed).

The module estimates the BER in digital direct transmission systems. The estimation can be performed assuming Gaussian or Chi-square statistics for the optical beat noise. The BER_OOK_Stoch module combines stochastic and deterministic approaches for the variance of the detected optical beat noise, and the mean values of 'one' and 'zero' signals are determined from the statistics of the input signal.

The estimation method chosen is the Chi-square approximation due to the origin of the system's noise. The threshold level is determined as the most optimum to achieve a good performance, and the original sequence is introduced in the module through a logic channel.

As every software platform, VPI photonics has its own limitations and some 'rules' must be followed. The combination of these limitations and the initial unfamiliarity with the software has brought a steep learning curve. Moreover, it has caused great difficulties in, apparently, very easy tasks. The greatest prime factor limit, the requirement to have an integer-number of samples per bit, the obligation in all the inputs of a module to have the same bandwidth or the problems with the bitrate and the N-QAM data generation, reception and analysis have delayed the simulation process and, in some cases, have impeded other interesting analysis inside the designs. Some of these studies have been proposed for future lines.

4.2 Conventional 10 Gbps NRZ OOK RoF Link

In order to compare the different systems performance, a RF transmission scheme is presented. In [33] a 24 Gb/s CAP-64QAM RoF system over 40-GHz transmission is proposed and demonstrated. The transmission scheme indicated is based on this system. With the intention of making easier the comparison the system is simplified. In this way, the data transmitted will be 10 Gbps NRZ OOK and the wireless transmission will not be included.

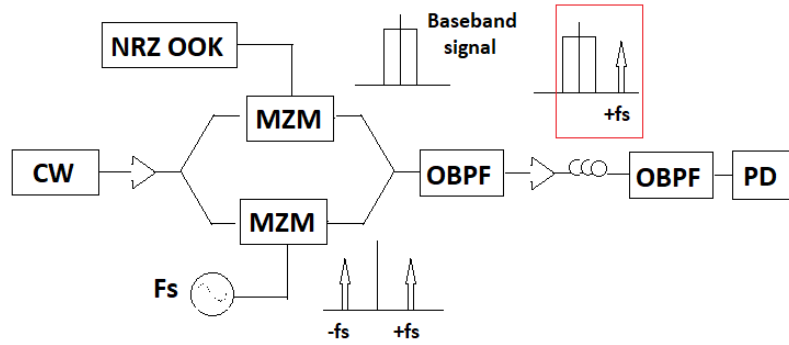


Figure 18. Schematic diagram of the proposed transmission system

Figure 18 shows the RoF signal modulation and mm-wave generation architecture. Optical Carrier Suppression (OCS) method is employed to generate the mm-wave as the system is easy to configure and it has a good performance. This method is the fundamental pillar of all the system, and is the main advantage of MWP techniques for mm-wave generation. The process works as follow: when biasing the MZM at the null point, the light source is modulated so that the carrier is almost suppressed and double sidebands appear at the frequency (f_s) which drives the MZM, so the separation between them is the double of that frequency. When the signal beats the photodiode a carrier at $2f_s$ is generated.

Besides the MZM for mm-wave generation, other MZM is used to modulate the signal. A continuous-wavelength (CW) light is the optical source and it is split into two arms in the I/Q modulator. This modulator consists of two MZMs placed in parallel, and a phase shifter in the lower arm. The upper arm is for the NRZ OOK modulation, while the other is for the mm-wave generation through OCS. For the OCS the MZM is biased at the null-point and the MZM is driven by a f_s RF signal. After joining both signals, the resulting signal is filtered with an optical band-pass filter (OBPF) that will keep the base-band signal and the first-order tone. The other undesired tones are cut off, so the frequency spacing between the base-band signal and the first-order tone is f_s . In this way, when the signal beats the photodiode, the mm-wave is generated at f_s , ready to be wireless transmitted. As indicated in the paper, the laser linewidth has no obvious impact on the results as the outputs of the two arms are from the same light source and only intensity modulation is used in each arm. To analyse the system's BER, the signal is down-converted to base-band.

To simulate with VPI, an experimental scheme of 10 Gbps NRZ OOK RoF system over 2.5-km SSMF 30 GHz transmission is shown in Figure 19.

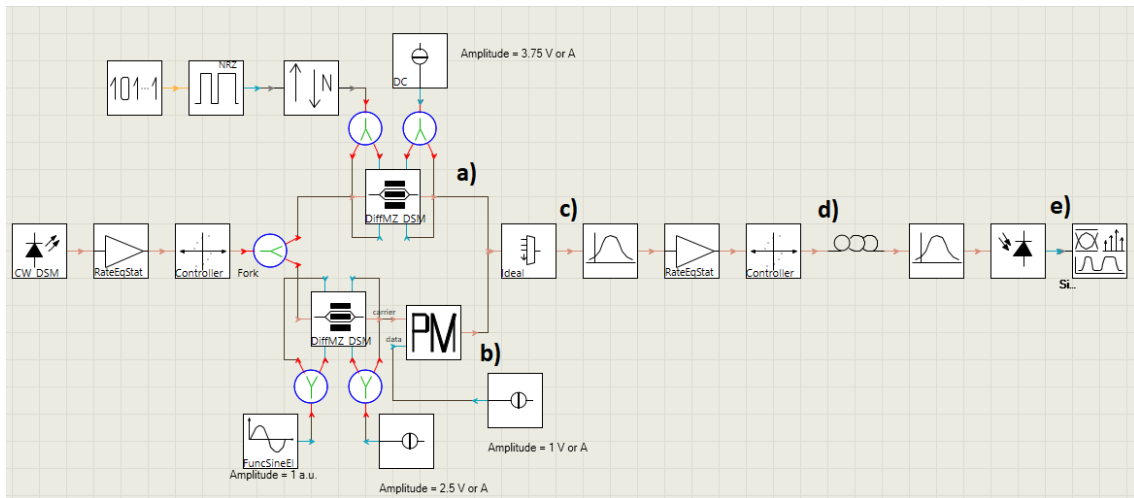


Figure 19. Schematic of a 10 Gbps NRZ OOK RoF system over 2.5-km SSMF 30 GHz transmission

The laser source and the MZMs are described in the beginning of the chapter. The I/Q modulator is available with two parallel MZMs. The upper arm is driven by the 10 Gbps NRZ OOK signal. It is generated via a binary sequence mapped to the 2 level OOK with a NRZ module. The bandwidth of the signal is 20 GHz. As the signal bandwidth and the optical source bandwidth are different a resample is necessary before the MZM. To modulate the signal, the MZM is biased at the quadrature point. As it has been said, the MZM in the lower arm operates in OCS condition to mm-wave generation. Then, the MZM is biased at the null point (2.5 V) and driven by a 30-GHz RF signal. The output of the MZM suffers a phase shift and both arms are coupled.

Figure 20, Figure 21 and Figure 22 show the optical spectrum of the output of lower arm MZM with mm-wave tones, the output of upper arm MZM with base-band signal and their union. From Figure 20 we can see a carrier suppression result with more than 25-dB first-tone to carrier power ratio.

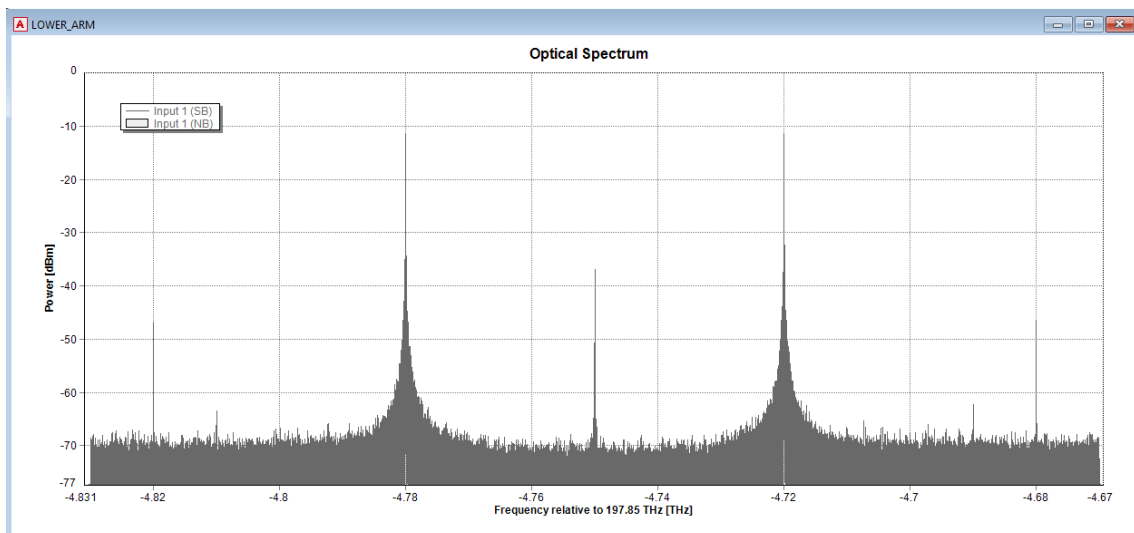


Figure 20. Optical spectrum at b)

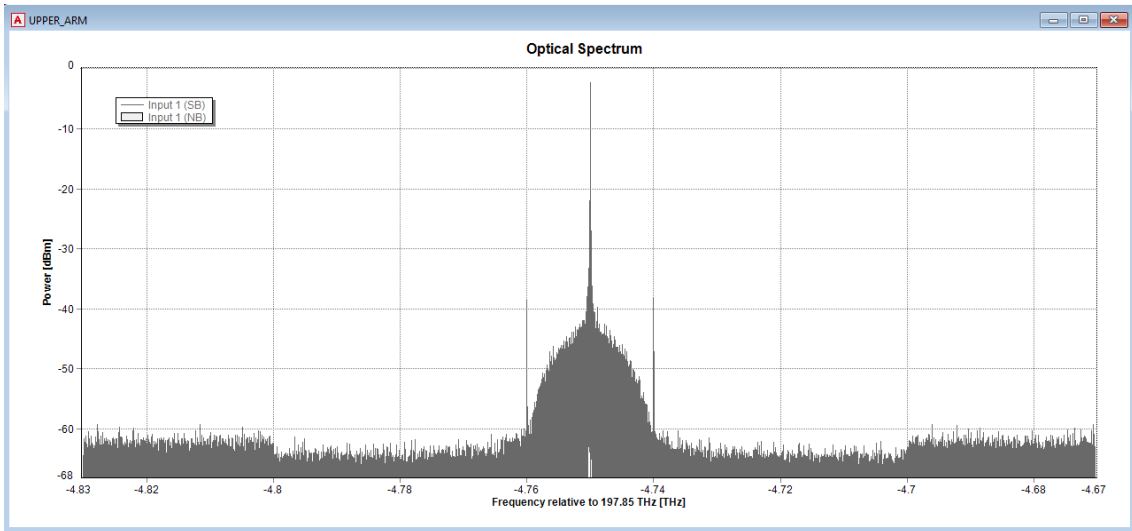


Figure 21. Optical spectrum at a)

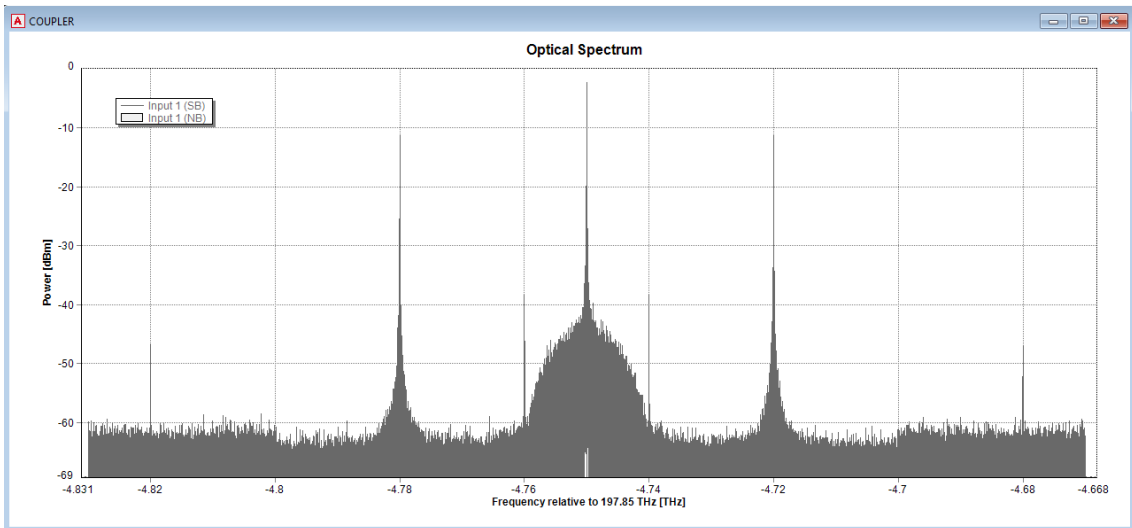


Figure 22. Optical spectrum at c)

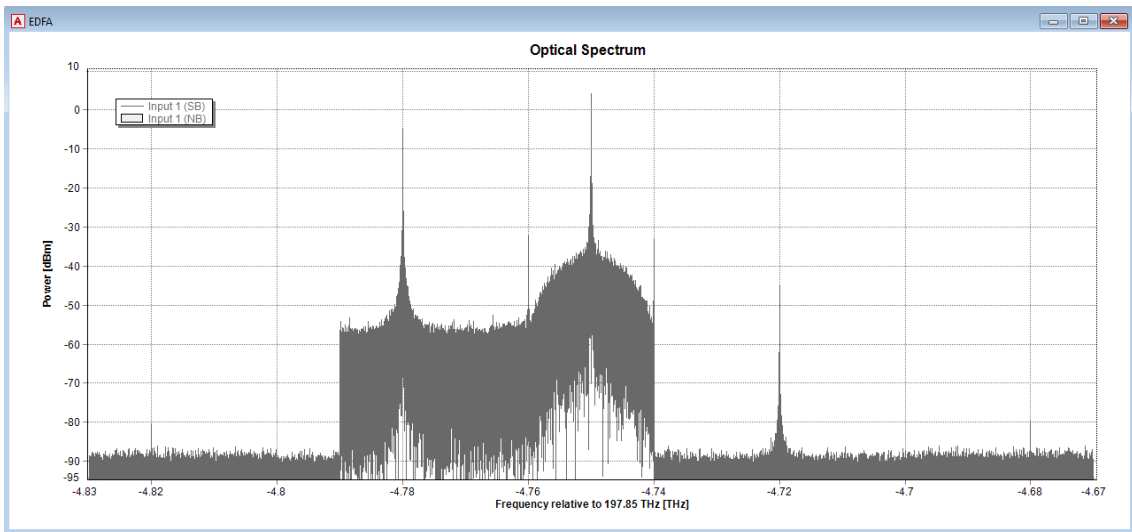


Figure 23. Optical spectrum at d)

Before penetrating in fiber, the signal is filtered with an OBPB and amplified by an EDFA. The OBPB keep only the left side-band first order mm-tone and the base-band signal with carrier spacing of 30 GHz (Figure 23). The power ratio of the carrier to base-band (CSR) is about 10-dB.

The EDFA is employed before the fiber to compensate the fiber loss. Once the signal is amplified, it is launched into the 2.5-km SSMF, which has about 5 dB loss at 193.1 THz. Then, the mm-wave signal is filtered again to reduce undesired components, as the ASE noise introduced by the EDFA, and up-converted by the photodiode.

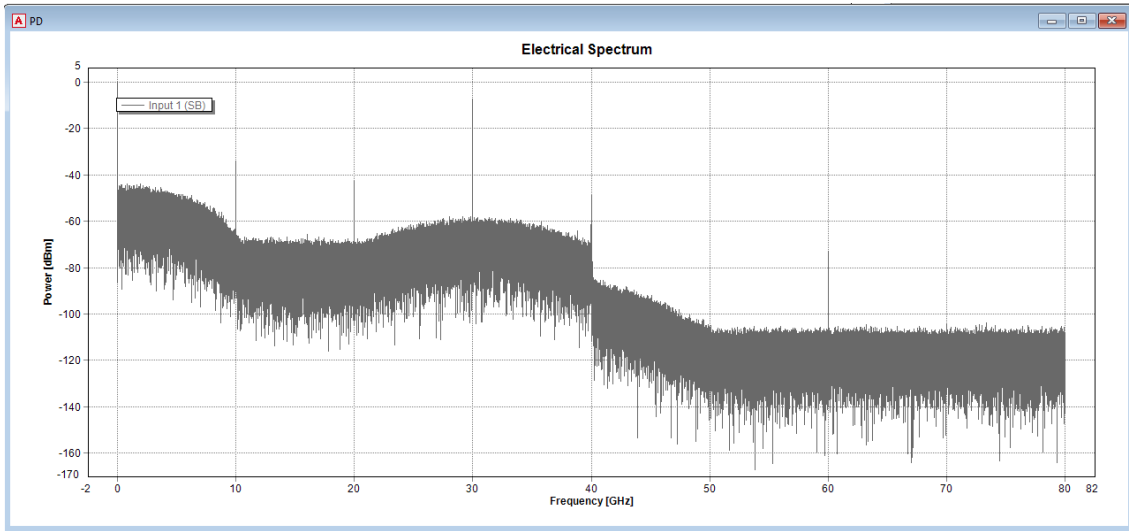


Figure 24. Electrical spectrum of the received 10 Gbps NRZ OOK mm-wave signal at 30 GHz

To compare the received signal with the transmitted ones, the signal is down converted to base-band by multiplying with a sine function. Then a BER analysis is executed. Figure 25, Figure 26, Figure 27 and Figure 28 show the optical spectrum of the down-converted signal, the waveform of the received sequence, the waveform of the original sequence and the BER results with 2 different speeds (5 and 10 Gbps). The results are very poor as the lowest BER level is $1e-3$ at 10 Gbps and $1.311e-5$ at 5 Gbps with a measured receiver sensitivity of -25 dBm.

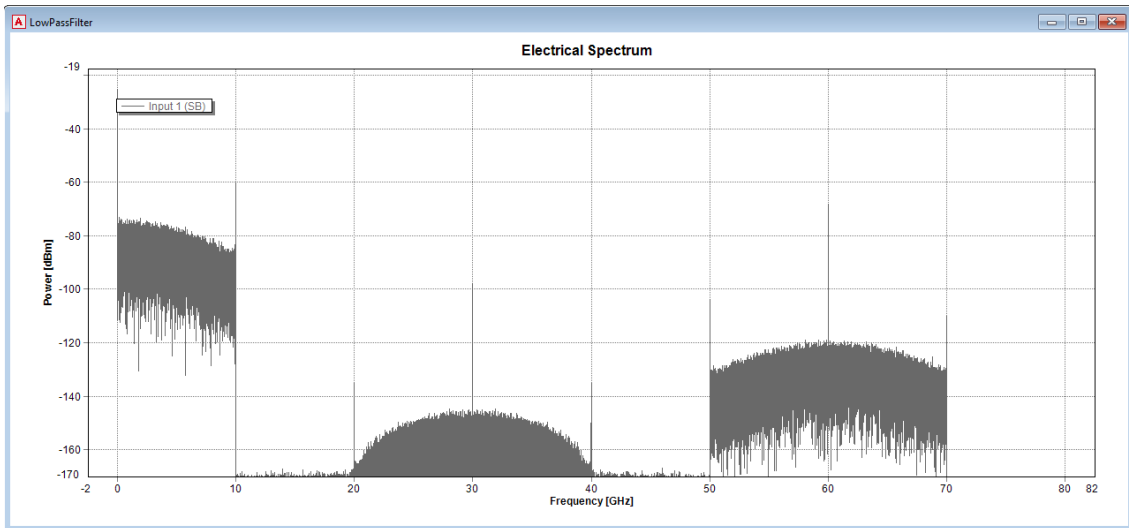


Figure 25. Electrical spectrum of the down-converted base-band 10 Gbps NRZ OOK signal

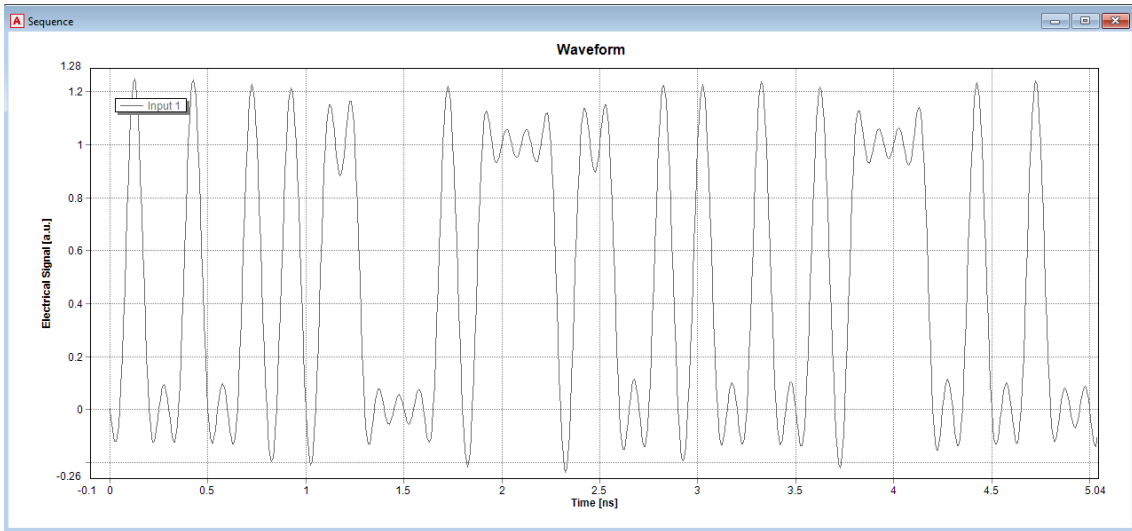


Figure 26. Original NRZ OOK transmitted sequence

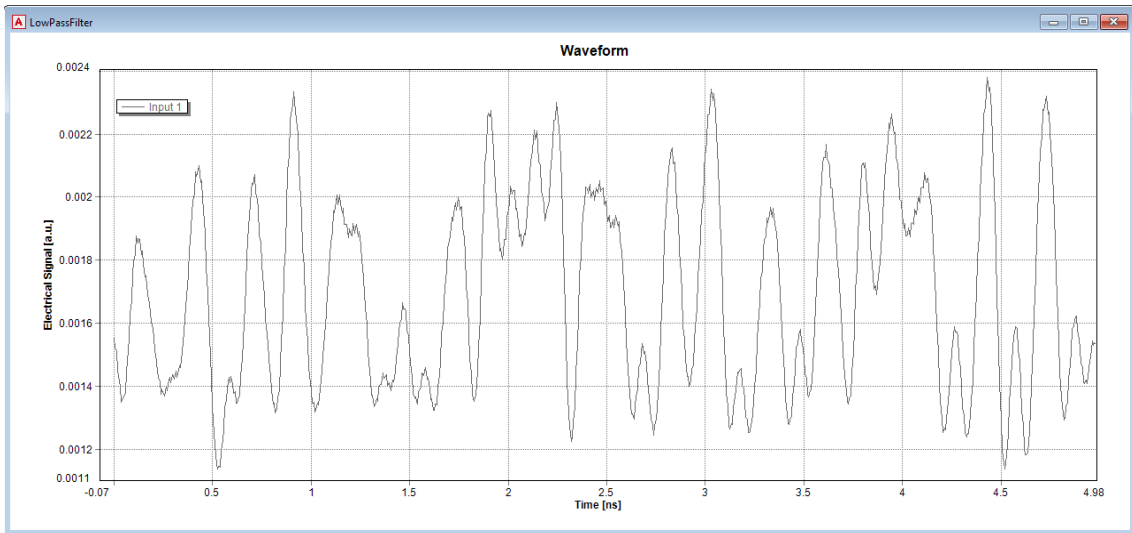


Figure 27. NRZ OOK received sequence

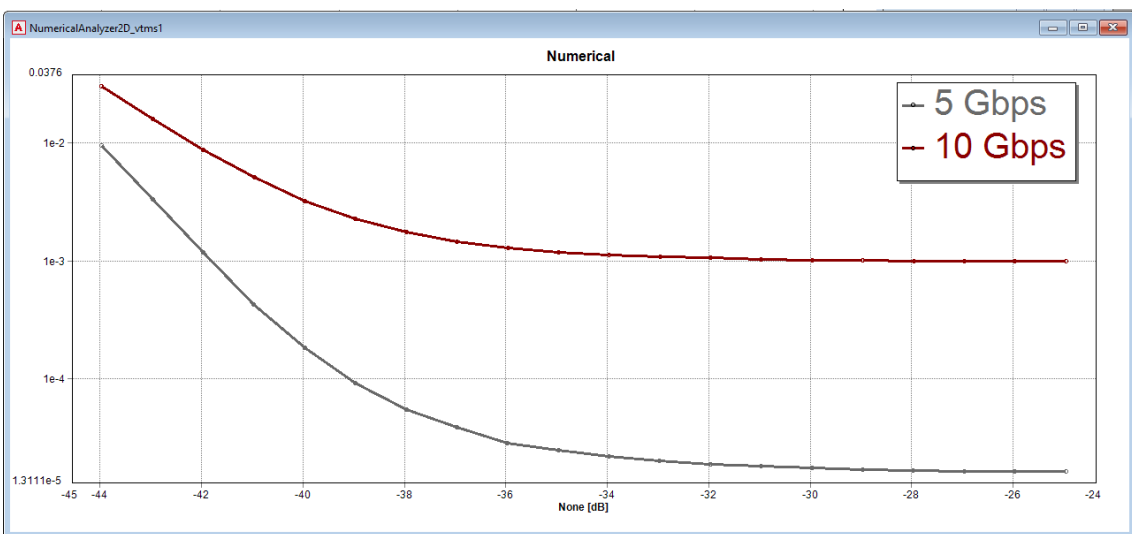


Figure 28. BER vs Received Optical Power for 10 and 5 Gbps NRZ OOK sequence

Concerning to the quality of the mm-wave generated, the system has been tested without data transmission. The MZM in charge of the data modulation is deactivated and the electrical spectrum obtained is the showed in the next figure. With -10 dBm RF power level, the signal

presents a SNR level of approximately 50 dB and the power difference with the first harmonic is almost 60 dB.

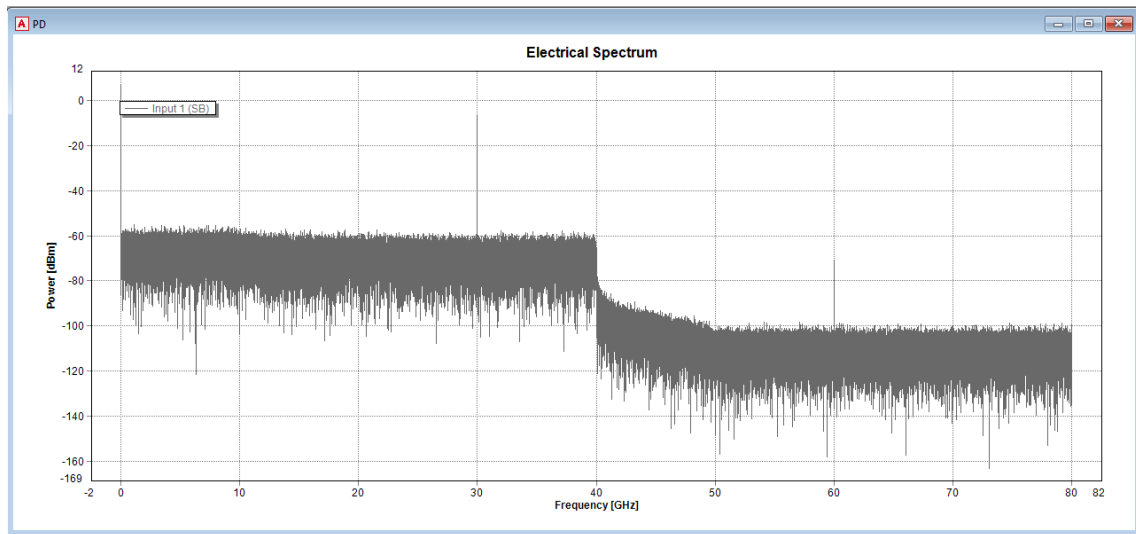


Figure 29. 30 GHz mm-wave generation

4.3 Microwave Photonics based 10 Gbps NRZ OOK RoF Link

Now that the transmission design has been described it is the turn to present alternative designs. The next design is the current most basic scheme to achieve mm-wave generation through microwave photonic techniques, and it is based in the system proposed in [34]. The most important contribution of this scheme in comparison with the previous design is the use of oscillators with the half frequency. While in the preceding system it is necessary a fs oscillator to transmit the data in a fs mm-wave signal, here the required oscillator frequency is the half to transmit the same data at the same frequency.

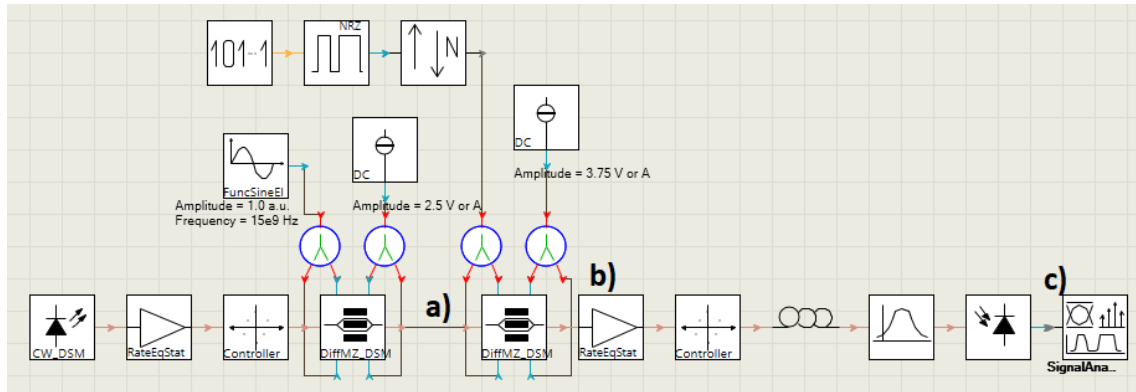


Figure 30. Alternative schematic of a 10 Gbps NRZ OOK RoF system over 2.5-km SSMF 30 GHz

Figure 30 shows the configuration of a 30 GHz radio-over-fiber NRZ OOK link system. In general, it consists of an optical carrier generation unit, a broadband data modulation, a fiber link and an optical receiver. As the previous design, it needs two MZM, one for the mm-wave generation and the other for the modulation, but they are not placed in parallel but in serial. The process to obtain the mm-wave through the first MZM is the same as the transmission design: the light from the laser source is modulated into the MZM biased at null-point (V_{π}) to generate an optical double-sideband signal with suppressed carrier (DSB-SC). The MZM is driven by a 15 GHz oscillator. The optical carrier suppression is approximately 26 dB (Figure 31).

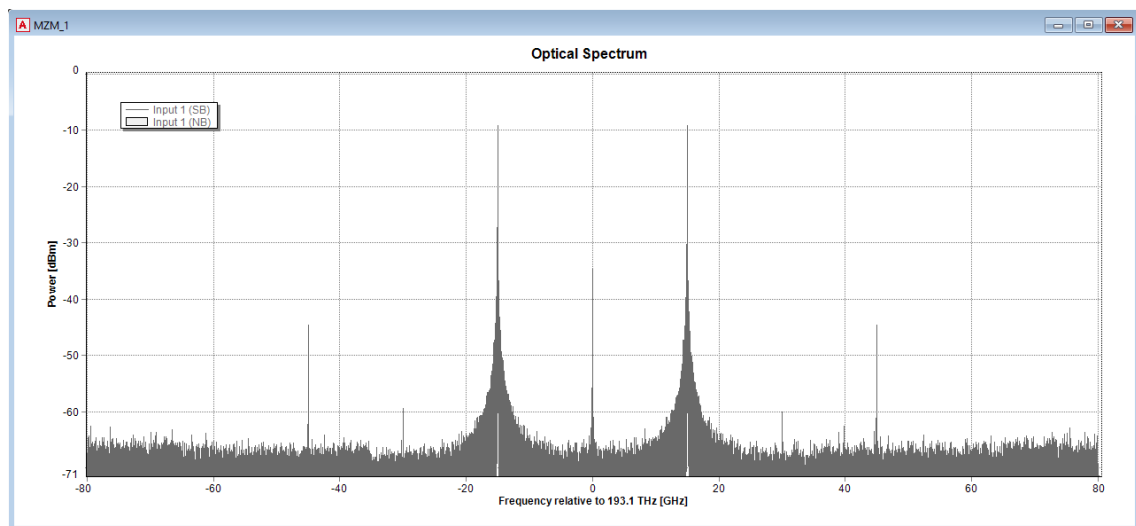


Figure 31. Optical spectrum at a)

Via the second MZM the optical carrier is modulated with NRZ OOK data by biasing the modulator to the quadrature point. A PRBS generator and a NRZ modulator produce the 10 Gbps and 20 GHz bandwidth signal. Figure 32 show the data modulated over the optical carrier.

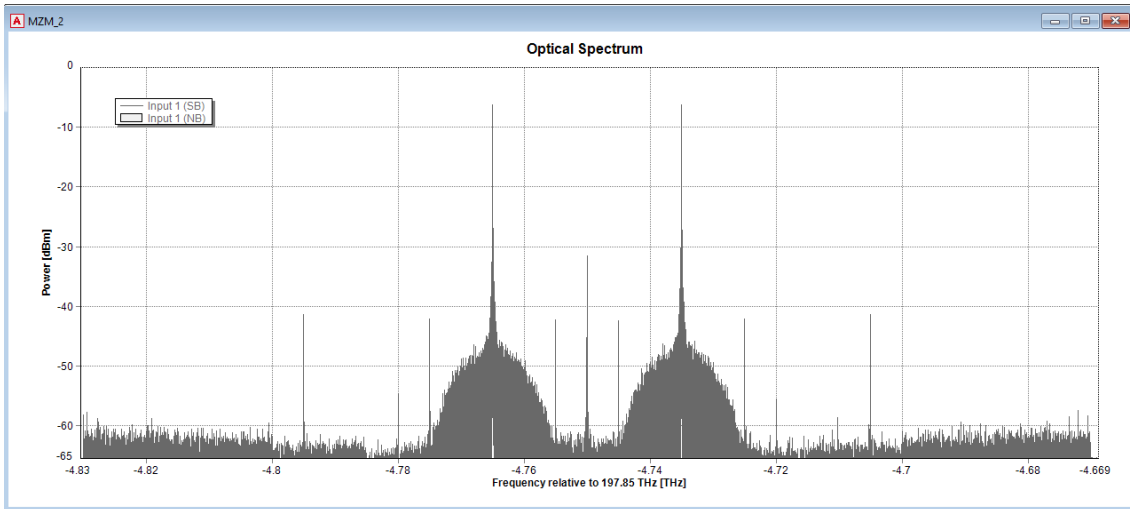


Figure 32. Optical spectrum at b)

The data-modulated mm-wave signal is amplified by an EDFA and transmitted through a 2.5 km SSMF. In order to get a better result, the mm-wave signal is filtered with an optical band stop filter which reduce the carrier level. The reason to employ a band stop filter instead of the band pass filter is that the results obtained are better. Moreover, the central carrier is the undesired component with the highest level.

The output is o/e-converted by a photodiode giving as result a 30 GHz 10 Gbps NRZ OOK signal as shown in Figure 33. In the figure, it can be appreciated the base-band data and the 30 GHz data.

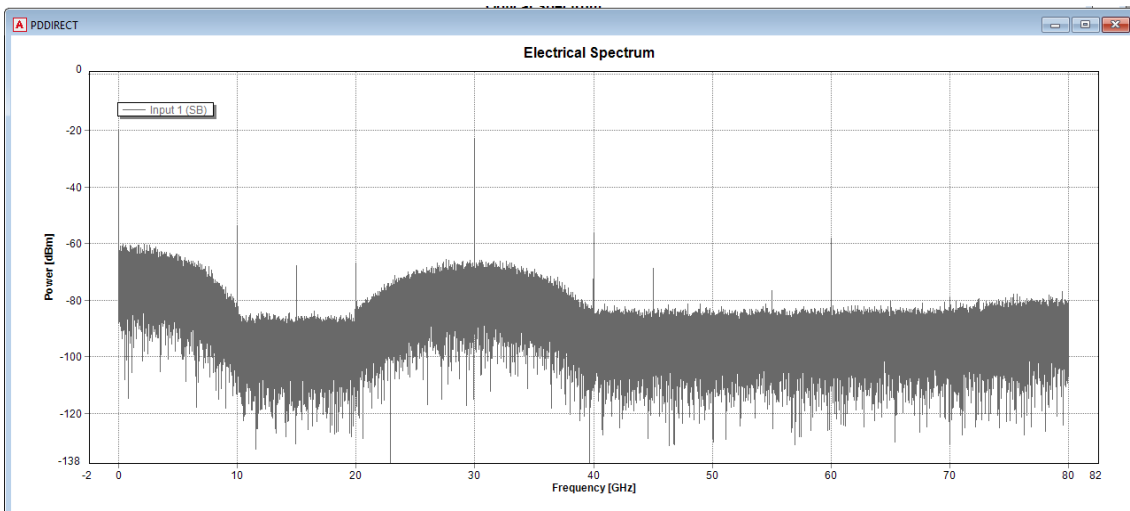


Figure 33. Electrical spectrum at c)

The signal is down-converted to base-band to be compared with the original sequence. The process is as in previous design by multiplying with a sinusoidal source with a frequency level of 30 GHz. The next figures show the original sequence and the resulting one.

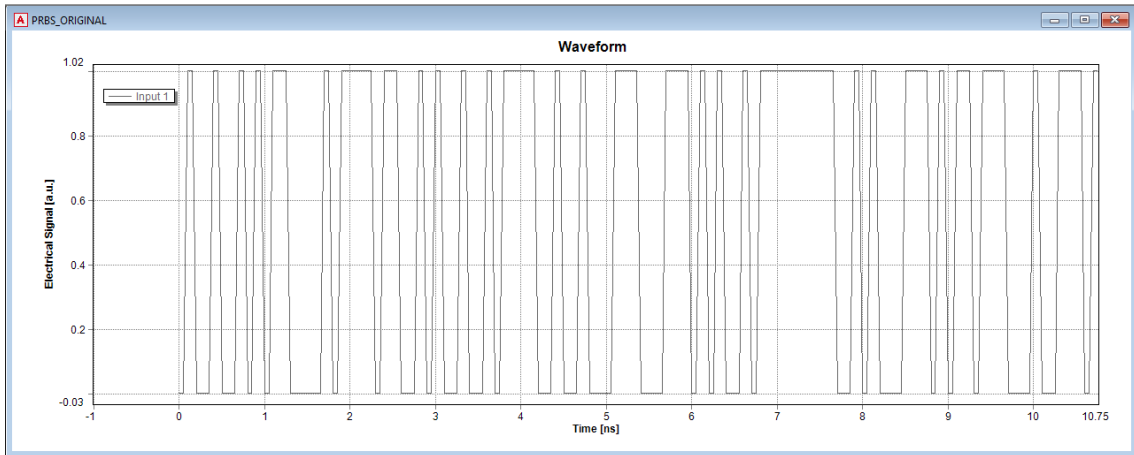


Figure 34. Original NRZ OOK transmitted sequence

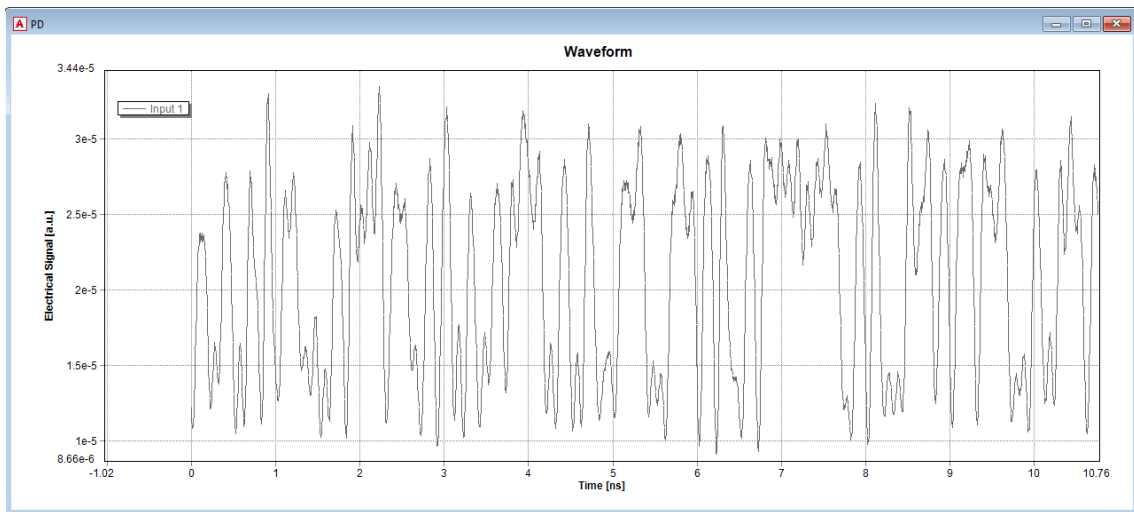


Figure 35. NRZ OOK received sequence

In order to analyse the system performance and how some parameters affect its behaviour, BER results versus receiver optical power are represented. The parameters studied are the data bit rate (Figure 36) and the mm-wave signal frequency (Figure 37).

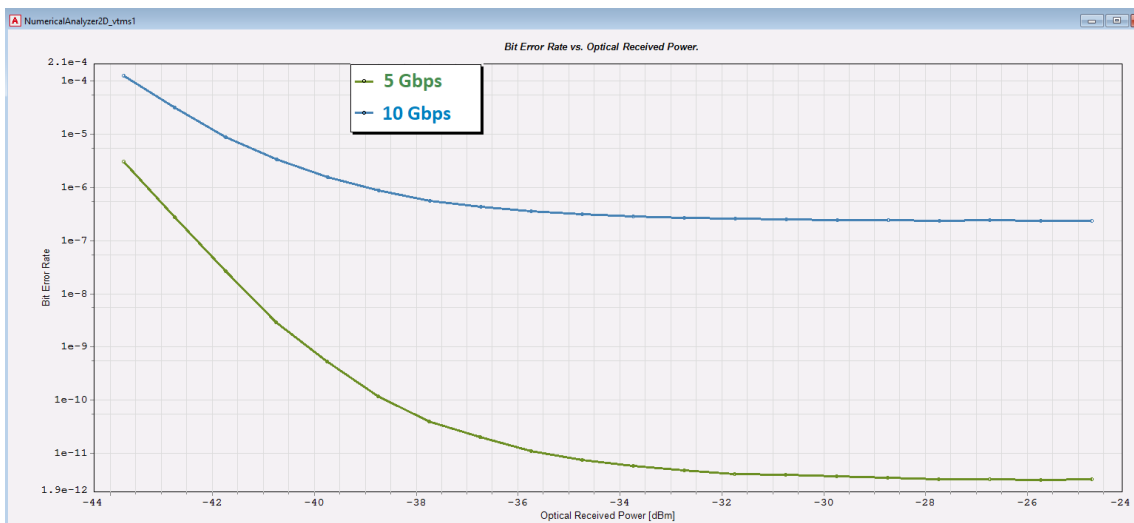


Figure 36. BER vs Received Optical Power for 10 and 5 Gbps at 30 GHz

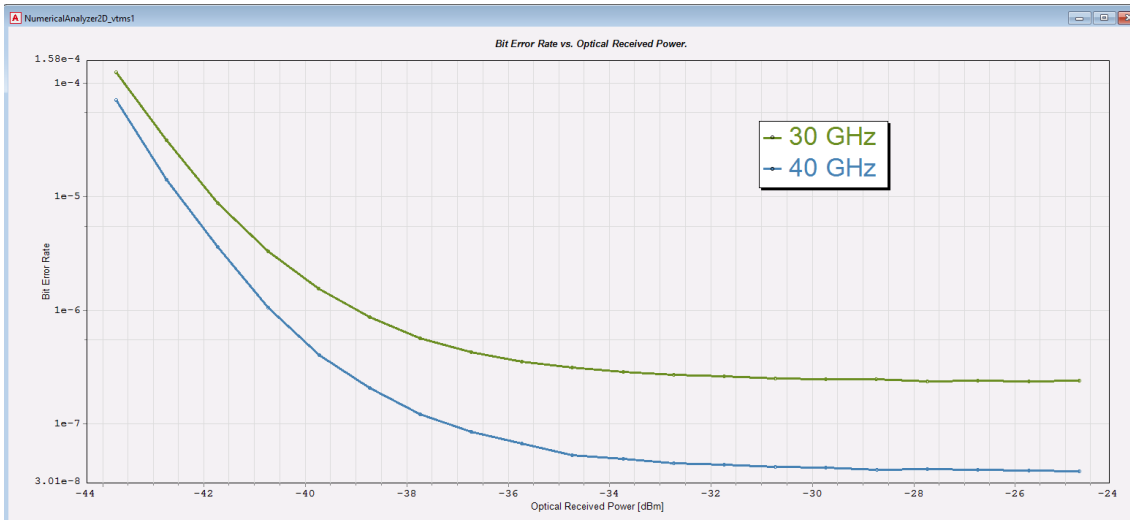


Figure 37. BER vs Received Optical Power for 30 GHz and 40 GHz signal at 10 Gbps

The first graphic shows a clearly better performance when employing the half bit rate. A -25 dBm receiver sensitivity achieves a BER level of about 1.7×10^{-12} with 5 Gbps while 7.3×10^{-7} with 10 Gbps. In the case of the frequency, the curve slopes are very similar. The lower BER level (4×10^{-8}) at 40 GHz point a better performance when the sidebands separation is greater.

In order to analyze the mm-wave signal quality, the electrical spectrum of the carrier generated without data modulation is depicted in Figure 38. The signal has a power of -10.63 dBm, it presents a SNR of 60 dB and the power difference with the harmonic is almost 30 dB.

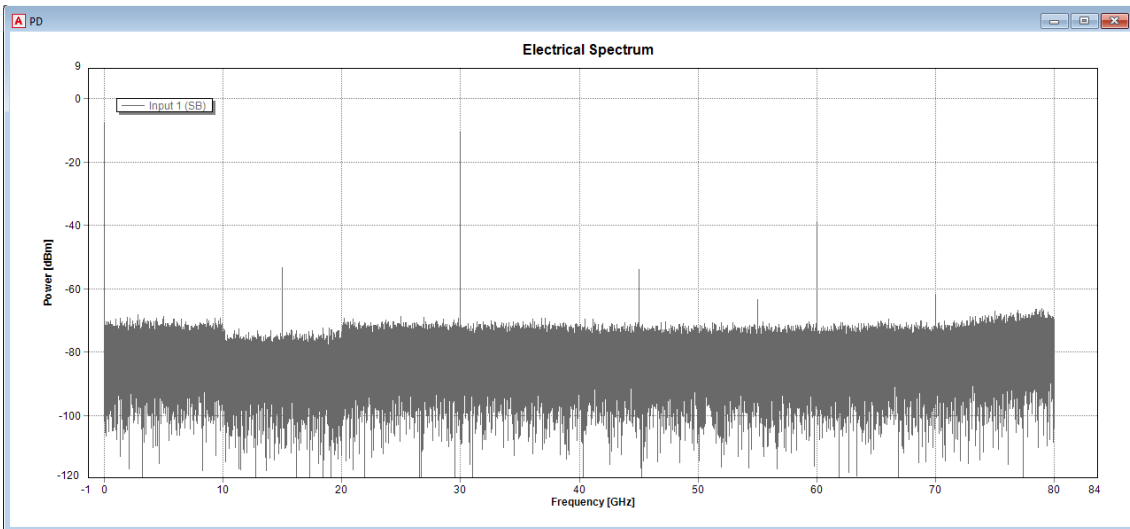


Figure 38. Electrical spectrum 30 GHz mm-wave signal

Now that both designs have been broken down, is the turn to compare them. Focussing in the data transmission, the MWP based design is significantly superior as the BER graphics demonstrate while the carrier figures of merits are very similar.

Besides, the design needs slightly less equipment. However, is the oscillator difference the most important aspect, as the feature and cost are extremely tied. The chance of utilizing an oscillator which the half frequency, in microwave frequency band is an aspect to take into account.

4.4 Optical microwave generator based on SBS with fine tunability

In section 3.3 several mm-wave generation schemes are introduced. Consequently, the fine tunability optical microwave generator based on SBS explained in section 0 is simulated.

As already noted, the system proposed in [27] revolves around a MZM biased at MITP to realize CS-DSB modulation and a frequency shifter based on SBS also (Figure 39).

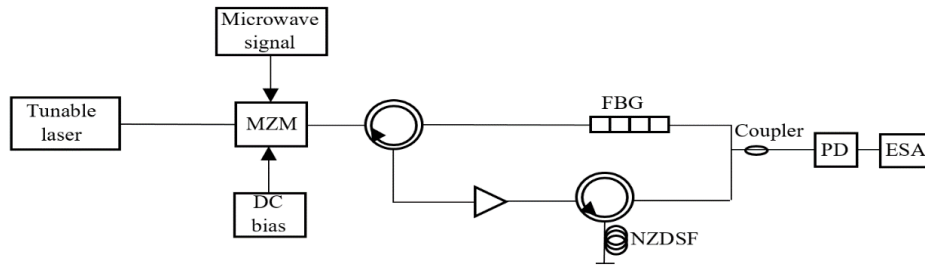


Figure 39. Schematic diagram of the proposed microwave generator

The light wave (f_0) is first modulated by the RF signal (f_m) in the MZM, realizing CS-DSB, and then, through a circulator and a Fiber Bragg Grating (FBG) the lower sideband is employed as a pump wave that stimulate the SBS process. A frequency shift module realized inside a None Zero Dispersion Shifted Fiber (NZDSF) with the SBS effect enlarge the frequency difference between the shifted lower sideband and the upper. Once the two components are coupled out and beat in a photo detector (PD), a microwave signal with a frequency equal to the frequency difference of the two sidebands is detected: $f_{RF} = 2f_m + v_B$. The system can be tuned by changing the frequency of the RF signal applied to the MZM.

The scheme developed in VPI photonics to simulate the system is the depicted in Figure 40.

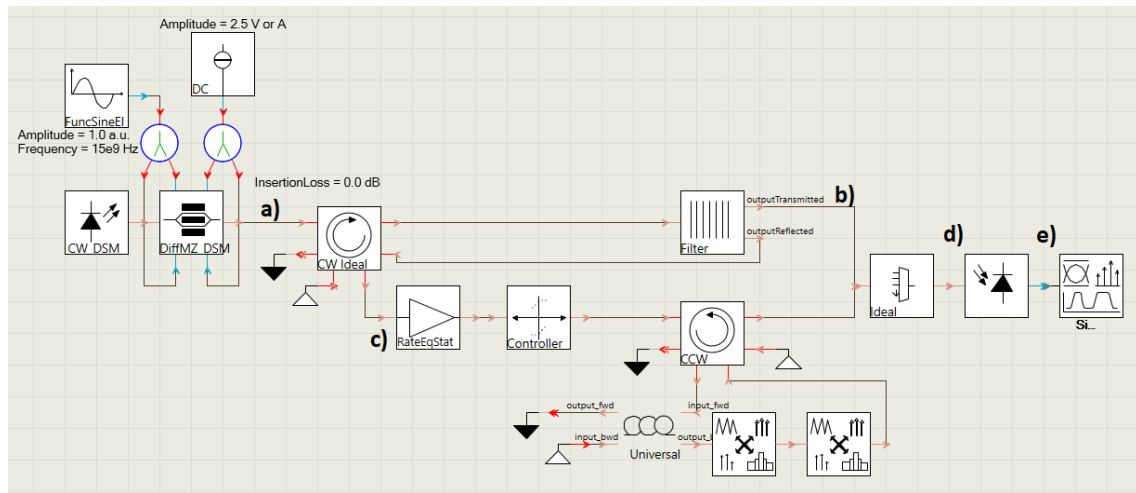


Figure 40. VPI photonics schematic of the proposed microwave generator

As noted, the light wave is modulated by a MZM biased at the null-point (V_{pi}) and driven by a sinusoidal source with a frequency and amplitude level of 15 GHz and 1 a.u. therefore, the result is the same as in previous design, a 26-dB optical carrier suppression.

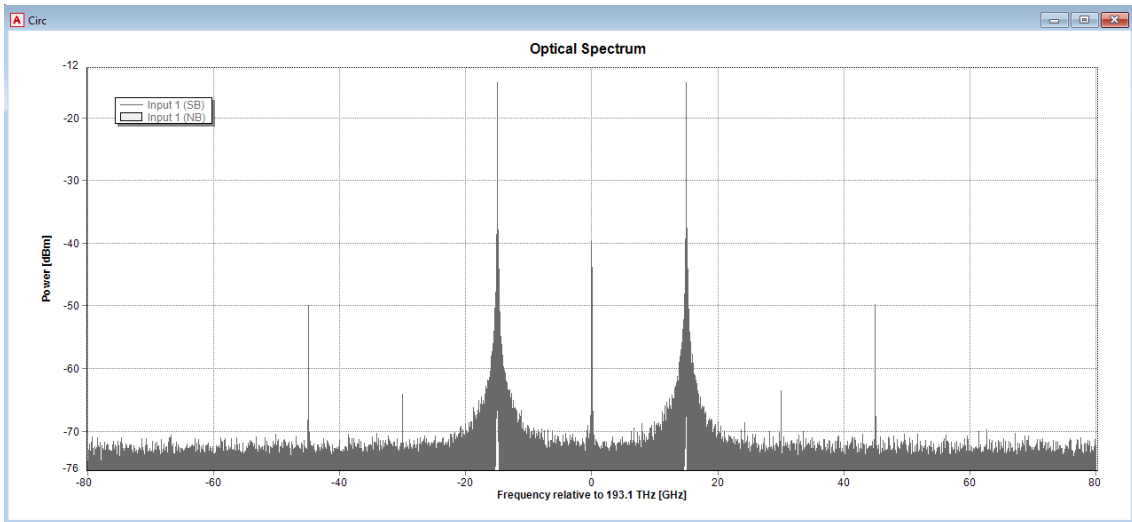


Figure 41. Optical spectrum at a)

The FBG filter handles the separation between the lower and the upper sideband. The first one is reflected to the circulator and amplified by an EDFA before entering in the frequency shift module.

The FBG frequency is set in 193.089 THz, the bandwidth is 50 GHz and the band rejection is 40 dB. In Figure 42 the filter parameter configuration is showed as well as its spectral response.

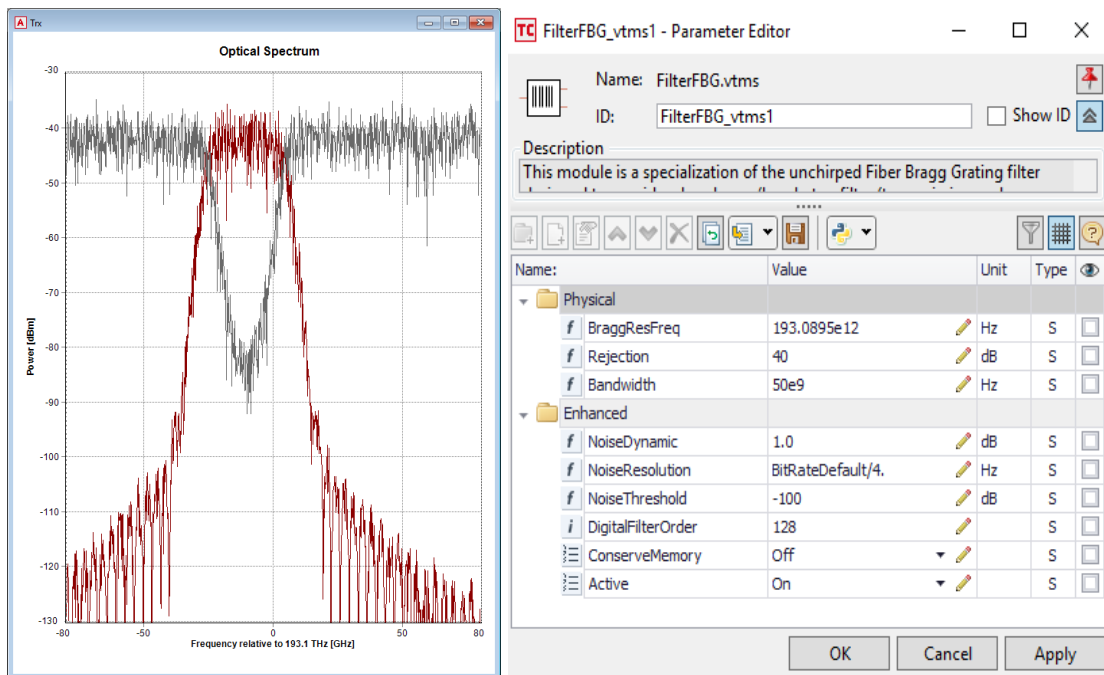


Figure 42. FBG filter parameters and characterization

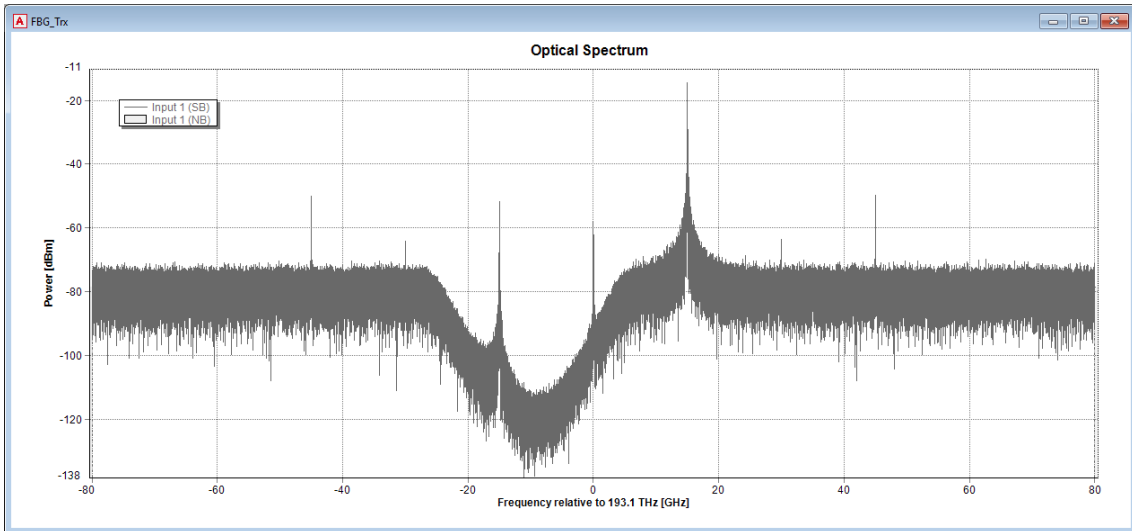


Figure 43. Optical spectrum at b)

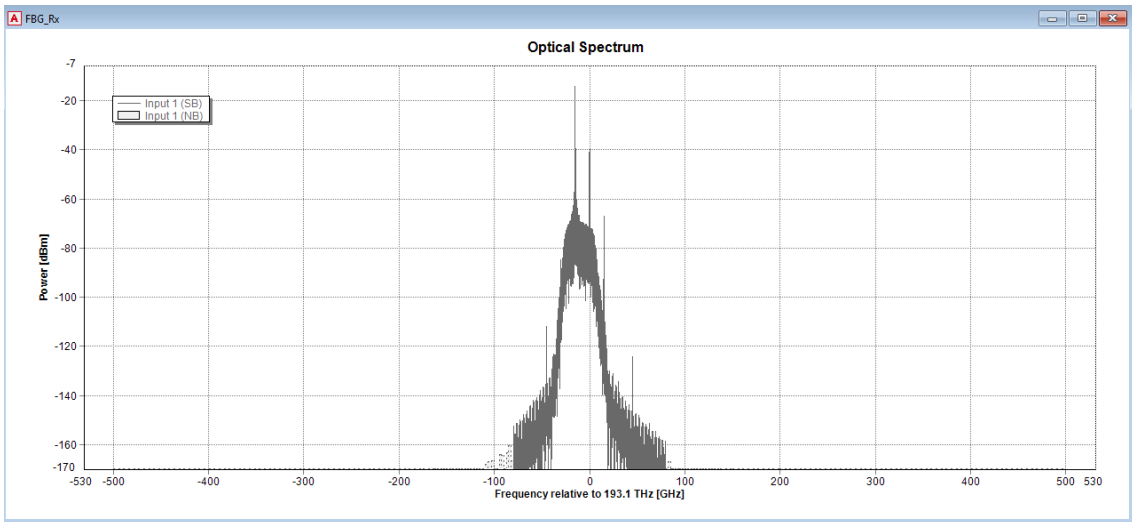


Figure 44. Optical spectrum at c)

The frequency shift module consists of a 10-km NZDSF. The SBS parameters are a 100-MHz bandwidth and a Stokes shift of 11 GHz. VPI Photonics works with diverse kinds of signals and it differentiates between Stokes signals and sampled band signal. So, a pair of converters are necessary or they will not interact. In the optical coupler, the upper sideband and the frequency shifted Stokes wave are coupled (Figure 45).

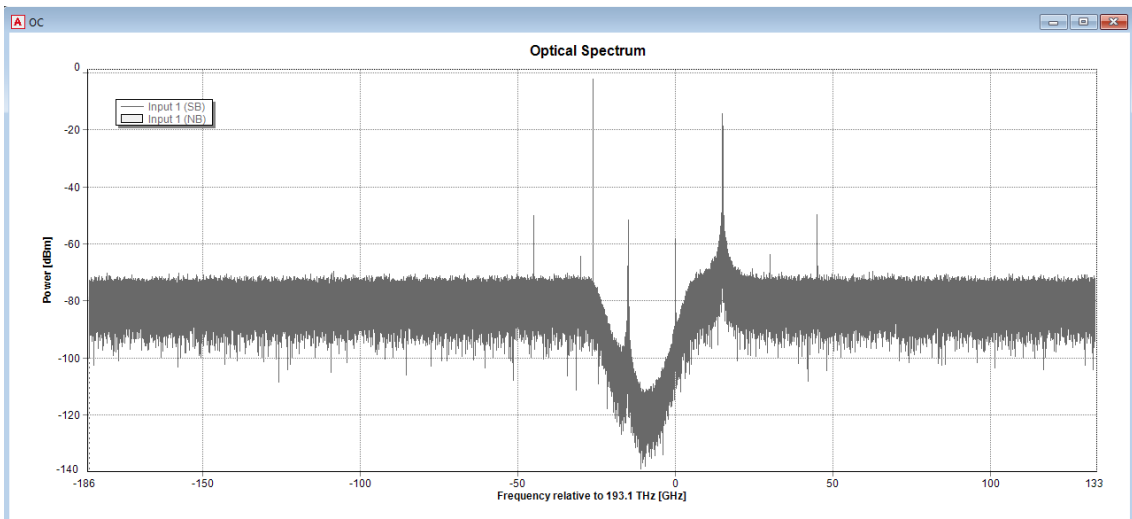


Figure 45. Optical spectrum at d)

The signal beats a photodiode and is o/e-converted. With a -38.72 dBm power, the mm-wave presents an approximately 50-dB SNR. The power difference with the highest undesired component is approximately 34 dB.

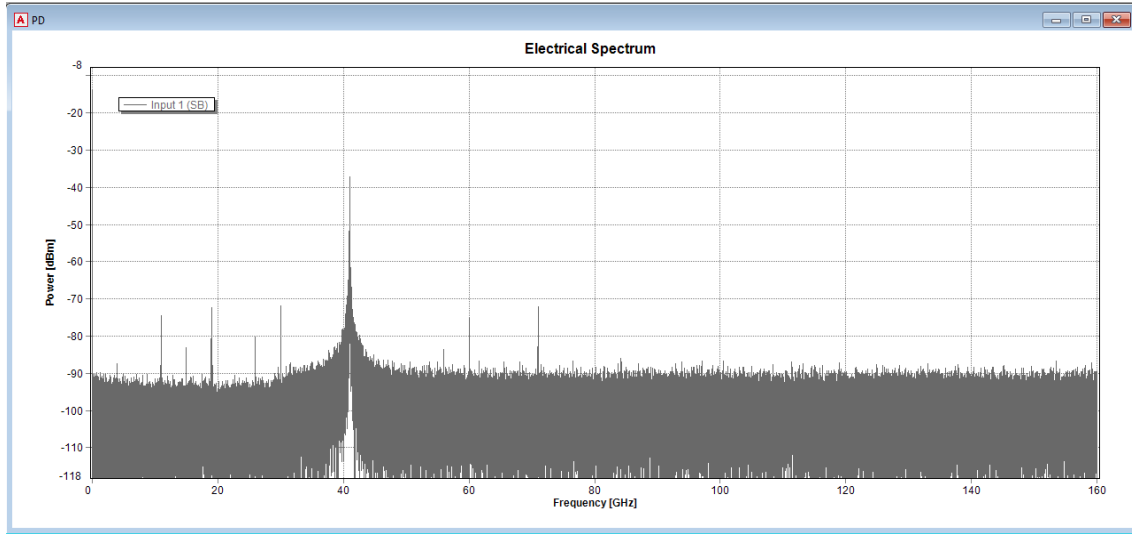


Figure 46. Electrical spectrum at e)

The system tunability has been tested with different driven frequencies and, as can be seen in Figure 47, the performance is not affected by the selected frequency.

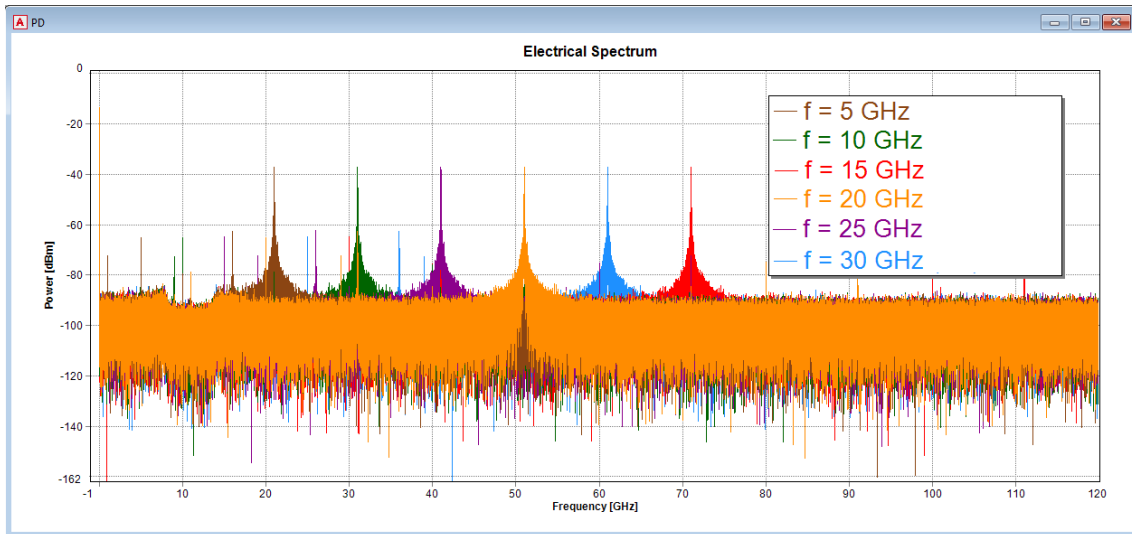


Figure 47. Electrical spectrum of 21 GHz, 31 GHz, 41 GHz, 51 GHz, 61 GHz and 71 GHz carriers

The process followed to test the tunability is the same as the realized in [27]. The modulation frequency applied to the MZM is varied between 5 and 30 GHz with 5 GHz steps. In the paper [27], is demonstrated that the central frequency of the system is given by:

$$f_{RF} = 2f_m + \nu_B$$

, where ν_B is the SBS frequency shift and f_m is the frequency applied to the MZM. The Stokes frequency shift is 11 GHz in the design. According to the formula, the Stokes shift and the oscillator frequencies employed, 21 GHz, 31 GHz, 41 GHz, 51 GHz, 61 GHz and 71 GHz carriers are obtained. It should be mentioned that the FBG center frequency must also be varied to be adjusted to the new sidebands separation.

In [27] the authors experimentally demonstrate the microwave generation with a SNR higher than 20 dB in the range from 14.67 GHz to 30.67 GHz. The simulation realized in the thesis also that SNR level and check the tunability between 21 GHz to 71 GHz.

4.5 Photonic generation of triangular-shaped microwave pulses using SBS-based optical carrier processing

Due to its interest and its use in signal processing, the photonic generation of triangular-shaped microwave pulses introduced in section 233.3.1 is also simulated.

Triangular-shaped mm-wave pulses are a waveform kind with only odd-order harmonics. Therefore, a MZM biased at the minimum-transmission-point (MITP) is used to generate only odd-order optical sidebands.

The schematic diagram of the generator proposed in [26] is shown in Figure 48.

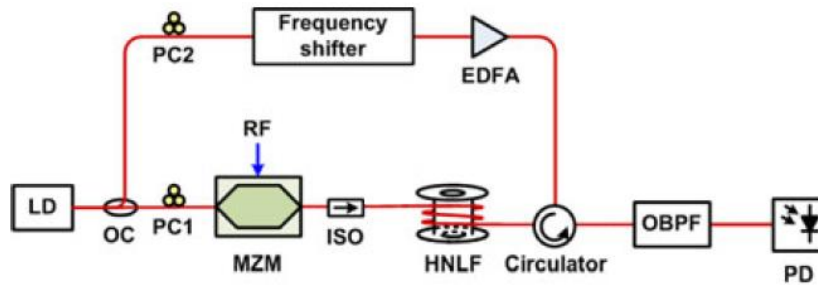


Figure 48. Schematic diagram of a triangular-shaped microwave pulses generator

As it was said, it consists of a laser diode (LD) whose light wave is divided into two parts by an optical coupler (OC). A frequency shifter raises the frequency of one part to operate as the pump of SBS. The frequency shift can be realized by using carrier-suppressed double sideband modulation. The other part is modulated in the MZM by a RF signal. The result is a light wave with only odd-order harmonics. The SBS pump light and the modulated light wave introduce themselves in a highly nonlinear fiber (HNLf) in opposite directions. Then the processing of the modulated signal using SBS is performed. An OBPF filter the unwanted optical sidebands leaving only the carrier and the 1st and 3rd order sidebands. The 2nd order harmonic can be neglected after the conversion in a PD.

Although triangular waveform consists of a large variety of odd-order harmonics, high order harmonics with fast roll-off factor have so insignificant impact that two odd-order harmonics are enough.

The scheme utilized to simulate the system in VPI Photonics is the following:

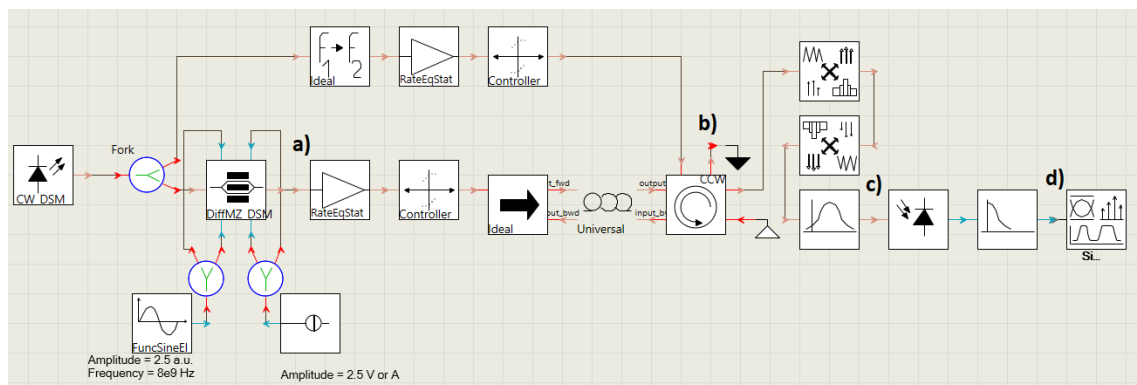


Figure 49. VPI Photonics schematic for the proposed system

As in the other systems, the light source is modulated in a MZM biased at the null point (Vpi). However, the frequency and amplitude level of the sinusoidal source that drives the MZM are different. The frequency level is now 8 GHz and the amplitude is 2.5 a.u. to achieve higher level harmonics. An amplitude of 1 a.u. gives very poor harmonics, very essential in this case. Here, the carrier suppression rate is approximately 35 dB. The modulated signal is amplified by an EDFA before entering in the 10-km HNLf.

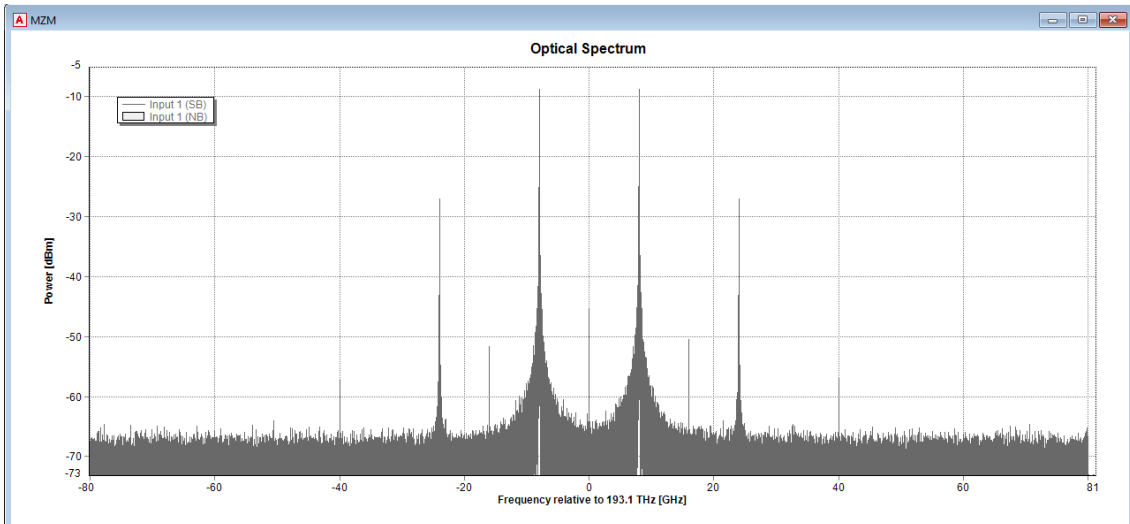


Figure 50. Optical spectrum at a)

The light wave in the upper branch is shifted to a higher frequency with a frequency shifter module. The frequency shift introduced is 11 GHz, the same as the Stokes shift. The output of the EDFA is utilized as pump wave.

Before entering in the HNLFF an isolator is employed to avoid that some signal reflection could damage components or alter their behavior. In the HNLFF, the previous SBS pump light is injected into, but in the opposite direction as the modulated light. The processing of the modulated signal using SBS is performed and it goes on to the circulator. As in the previous design, two converters are needed to allow the interaction between signals, obtaining the next signal (Figure 51). The figure shows a difference of about 5 dB between the power of the recovered optical carrier and the +1st-order sideband, and about 15 dB between the +1st-order and the 3rd-order sideband.

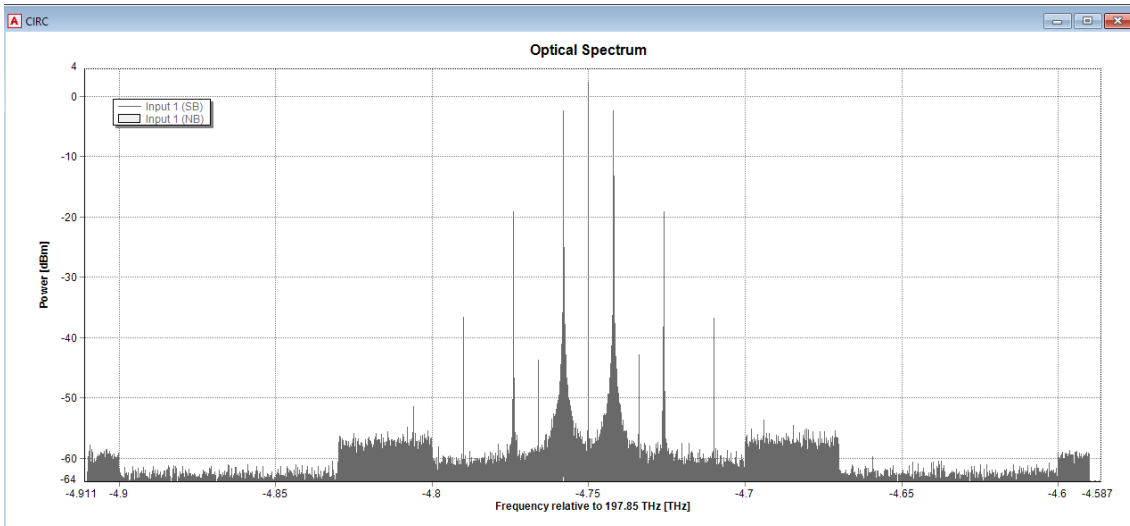


Figure 51. Optical spectrum at b)

However, the signal contains many unwanted components. They are filtered out by an OBPF which only leaves the carrier, the +1st-order and the +3rd-order sidebands. As the power of the optical carrier is much larger than of the +1st-order, the +2nd-order electrical harmonic can be neglected after the o/e-conversion.

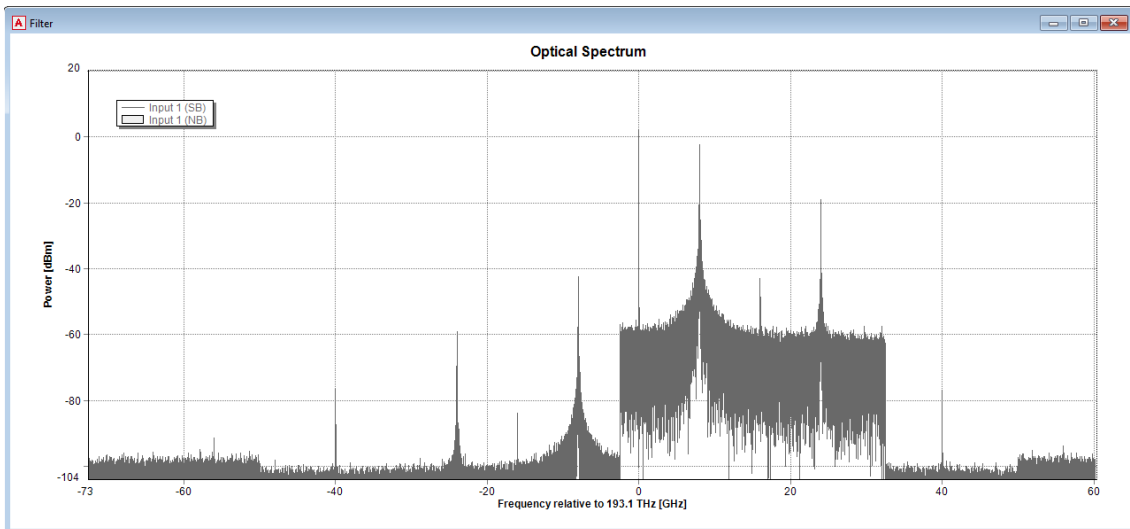


Figure 52. Optical spectrum at c)

An electrical bandstop filter filtered out the 2nd-order harmonic to improve the signal waveform. In Figure 53 and Figure 54 the frequency domain electrical spectrum and the waveform of the signal are depicted. The power of the 1st-order harmonic is about 19 dB higher than that of the 3rd-order harmonic.

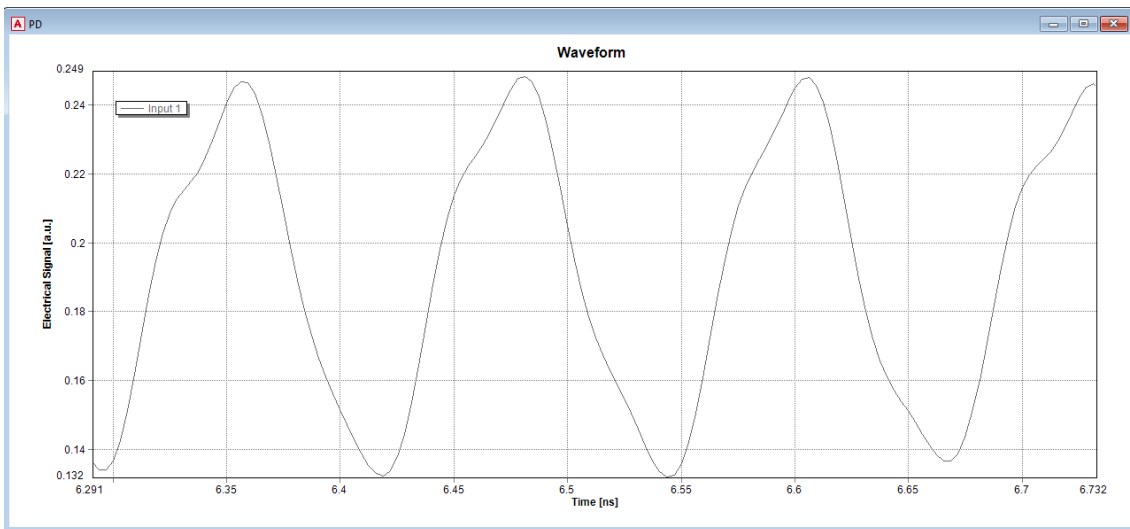


Figure 53. Waveform of the 8 GHz triangular-shaped pulses

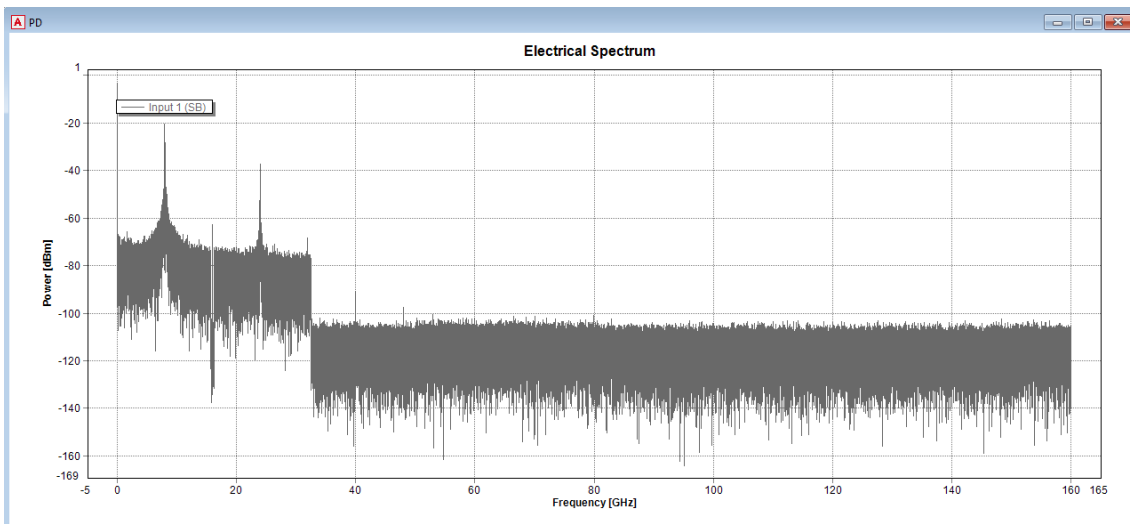


Figure 54. Electrical spectrum at d)

The tunability of the system is achieved through the variation of the RF signal frequency applied to the MZM. Hence, it results a stable generation system with fine accuracy in parameter control. As done in the paper, the tunability is studied at 5 GHz and 10 GHz too. The system also presents a correct performance at these frequencies.

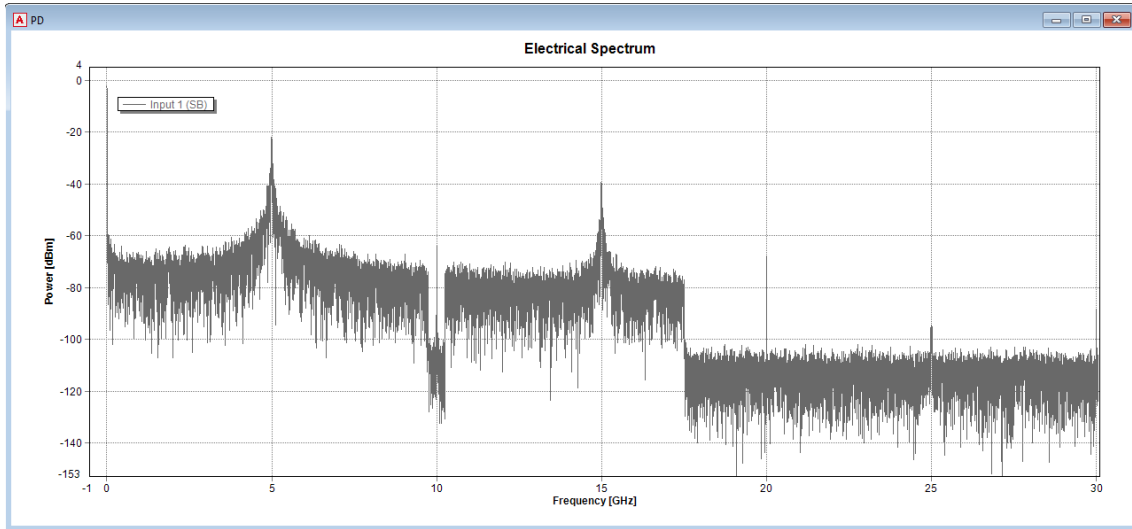


Figure 55. Electrical spectrum of 10 GHz triangular-shaped pulse

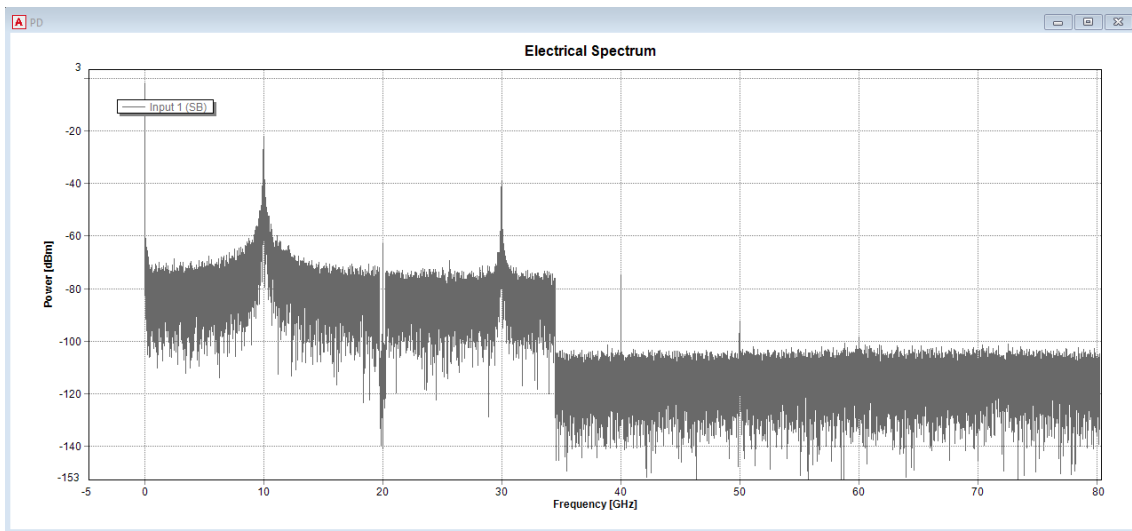


Figure 56. Electrical spectrum of 5 GHz triangular-shaped pulse

The results obtained show a RF power of -20.07 dBm in the 5 GHz signal, and 17.65 dB and 43.87 dB higher than the 3rd- and 2nd-order harmonics, respectively. The SNR level is about 57.13 dB. In [25] the SNR is approximately 60 dB, and the 1st- to 3rd-order harmonic power difference is 17.1 dB.

In the case of the 10 GHz signal, the power of the 1st- order harmonic is -20.54 dBm, 17.65 dB higher than the 3rd-order harmonic. In the paper is about 18.7 dB. Moreover, the SNR is 54.56 dB, almost the same as in the results obtained in the paper. Therefore, the experimental outcomes from [25] have been reached.

4.6 Flexible two lasers RF mm-wave generation system

All the previous designs allow to tune the frequency at which the RF signal is generated, however, the resulting frequency strongly depends on the oscillator's frequency applied to a MZM. The final frequency is always the same, the double or the double plus the Stokes frequency shift as the frequency applied.

In this section, a more flexible design is proposed. It is also based on the optical carrier suppression method realized with MZM, however, it employs two lasers to provide more flexibility.

When utilizing only a light source the mechanism to generate the carrier is as showed in the next illustration:

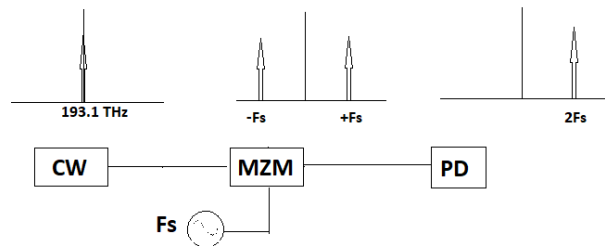


Figure 57. Schematic diagram OCS method

The proposed design employs this method but two lasers, and a subsequent filter of the sidebands desired:

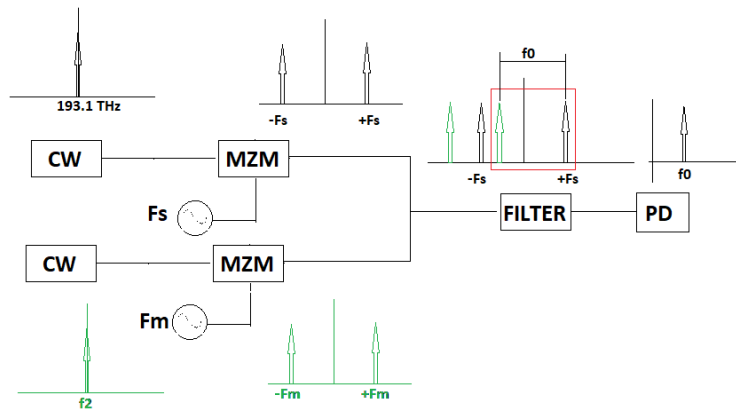


Figure 58. Schematic diagram of the proposed system

The mm-wave frequency can be tuned by changing the frequency in the oscillators utilized, by changing the emission frequency in the lasers or even by selecting a different combination of sidebands.

The VPI schematic utilized to demonstrate the system's feasibility is presented in Figure 59. The lasers, MZM and photodiode are the same that has been utilized throughout the thesis, but with a slight difference. One of the laser's emission frequency is set to 193.14 THz, 40GHz higher than the other.

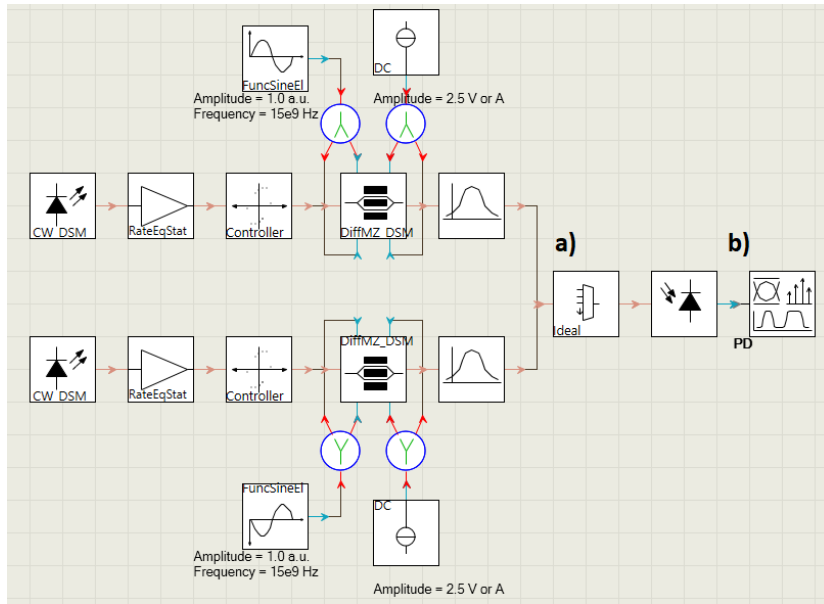


Figure 59. VPI photonics schematic for the proposed system

The light source of each laser is independently amplified by an EDFA. Then, the DSB-SC process is realized via the MZM. In this case, the frequencies that drive the MZMs are the same, but they can be completely distinct.

To provide an enhanced flexibility two OBPF deal with the filtering of the desired sidebands, so they do not need to be contiguous.

If none filtering were applied, the optical spectrum would be as depicted in Figure 60.

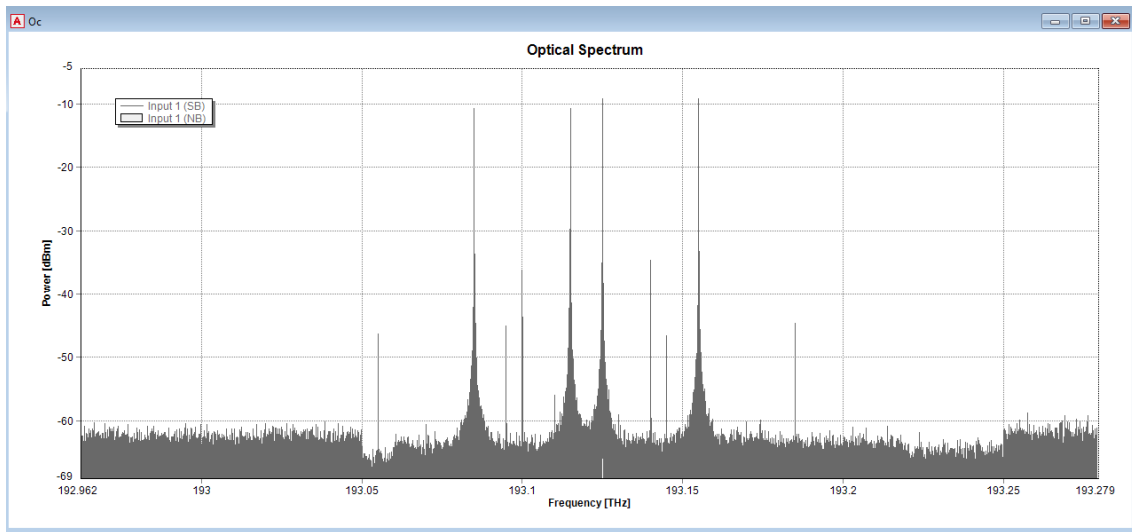


Figure 60. Optical spectrum at a) without filtering

The OBPF implemented are configured to filter out the furthest sidebands, the situated at 193.085 THz and the other at 193.155 THz. This means a sidebands separation of 70 GHz.

In Figure 61 the generated 70 GHz signal is depicted. The carrier has a RF power of -39.42 dBm. The power difference with the highest undesired component is about 21.7 dB. It is likely that the beating in the photodiode provides the signal waveform. So, the SNR is measured until the base of the carrier at -84.35 dBm instead of at -117.35 dBm, giving a 44.93 SNR.

This system must be studied, adjusted and perfectioned with more detail in the future in order to reach a better performance.

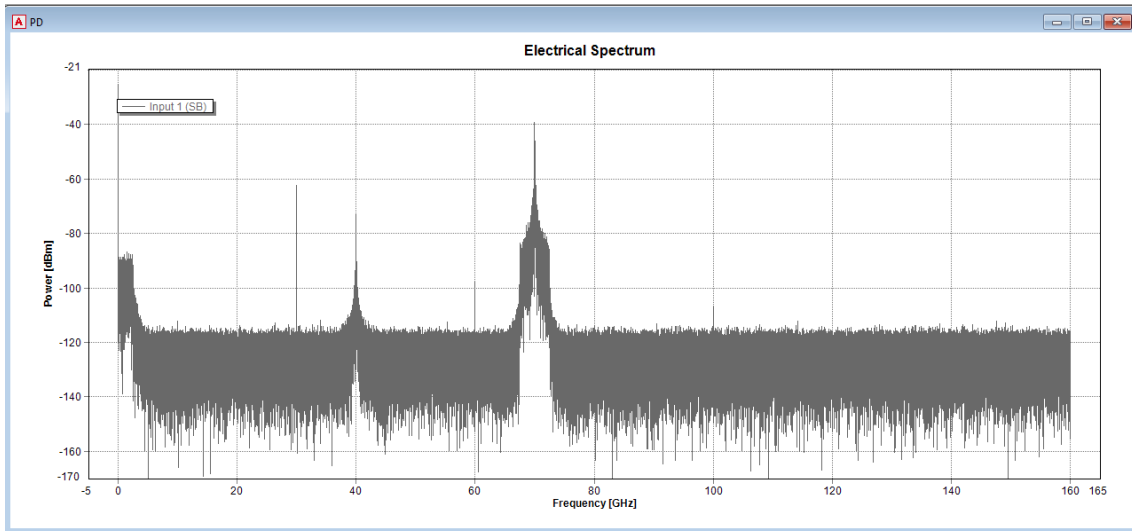


Figure 61. Electrical spectrum at b)

The main characteristic of this design is its enhanced flexibility, its cost is higher than others design because of the number of lasers required, however it could be of great interest in determined scenarios where the tunability is crucial.

Chapter 5. Budget

Once the designs viability is demonstrated, is the turn to talk about the cost of implementing such schemes. A very important aspect in a network deployment is the economic cost. The implementation speed and success of the new standard between the operators largely depends on this aspect. Therefore, a budget of every design is estimated to use it as an indicator of each design feasibility to be utilized.

In the following budgets, the photodiode receiver, the data generation and the fiber optic used to transmit the signal are not included as they are supposed to be the same in all the designs, and their price depends on the modulation format, the physical separation between the generator and the receiver, etc.

The optoelectronic components required for the designs and their prices have been extracted from the following web pages with the intention of calculating a primary budget: www.thorlabs.com [35], www.digikey.com [36] and www.mouser.com [37].

As showed with the next budgets, the MWP based link transmission design is the cheapest with a difference of about 2.000,00 € with the second cheapest design. Moreover, the designs described in section 4.4, 4.5 and 4.6 are the most expensive.

The MWP based design from section 4.3 has the following estimated budget:

	Quantity	Price	Total
<i>CW DFB Laser</i>	x 1	2490,00 €	2490,00 €
<i>EDFA</i>	x 2	3690,00 €	7380,00 €
<i>PC</i>	x 2	166,15 €	332,30 €
<i>MZM</i>	x 1	1998,00 €	1998,00 €
<i>15 GHz Oscillator</i>	x 1	36,73 €	36,73 €
<i>DC Source</i>	x 1	988,71 €	988,71 €
<i>OBPF</i>	x 1	84,75 €	84,75 €
<i>Total</i>			13310,49 €

Table 3. Estimation budget design from section 4.3

The conventional design from section 4.2 has the following estimated budget:

	Quantity	Price	Total
<i>CW DFB Laser</i>	x 1	2.490,00 €	2.490,00 €
<i>EDFA</i>	x 2	3.690,00 €	7.380,00 €
<i>PC</i>	x 2	166,15 €	332,30 €
<i>MZM</i>	x 1	1.998,00 €	1.998,00 €
<i>30 GHz Oscillator</i>	x 1	60,45 €	60,45 €
<i>DC Source</i>	x 1	988,71 €	988,71 €
<i>OBPF</i>	x 1	84,75 €	169,50 €
<i>Phase Shifter</i>	x 1	2.249,00 €	2.249,00 €
<i>Optical coupler</i>	x 1	3,86 €	3,86 €
<i>Total</i>			15.671,82 €

Table 4. Estimation budget design from section 4.2

The SBS based design with fine tunability from section 4.4 has the following estimated budget:

	Quantity	Price	Total
<i>CW DFB Laser</i>	x 1	2.490,00 €	2.490,00 €
<i>EDFA</i>	x 1	3.690,00 €	3.690,00 €
<i>PC</i>	x 1	166,15 €	166,15 €
<i>MZM</i>	x 1	1.998,00 €	1.998,00 €
<i>15 GHz Oscillator</i>	x 1	36,73 €	36,73 €
<i>DC Source</i>	x 1	988,71 €	988,71 €
<i>Circulator</i>	x 2	547,00 €	1.094,00 €
<i>Filter FBG</i>	x 1	427,50 €	427,50 €
<i>Optical coupler</i>	x 1	3,86 €	3,86 €
<i>10 km HNLf</i>	x 1	4.310,00 €	4.310,00 €
<i>Total</i>			15.204,95 €

Table 5. Estimation budget design from section 4.4

The fiber included in the budget is the employed to realize the frequency shift based on the SBS effect.

In the budget for the triangular-shaped pulses generator from section 4.5 the fiber required to produce the Stoke frequency shift is included:

	Quantity	Price	Total
<i>CW DFB Laser</i>	x 1	2.490,00 €	2.490,00 €
<i>EDFA</i>	x 2	3.690,00 €	7.380,00 €
<i>PC</i>	x 2	166,15 €	332,30 €
<i>MZM</i>	x 1	1.998,00 €	1.998,00 €
<i>15 GHz Oscillator</i>	x 1	36,73 €	36,73 €
<i>DC Source</i>	x 1	988,71 €	988,71 €
<i>Frequency Shifter</i>	x 2	2.082,75 €	2.082,75 €
<i>Circulator</i>	x 1	547,00 €	547,00 €
<i>10 km HNLf</i>	x 1	4.310,00 €	4.310,00 €
<i>OBPF</i>	x 2	84,75 €	169,50 €
<i>Isolator</i>	x 1	190,00 €	190,00 €
<i>Total</i>			20.524,99 €

Table 6. Estimated budget for the design from section 4.5

This is the most expensive system due to the frequency shifter module, realized with the double sideband carrier suppression method and a OBPF.

The budget of the two lasers design is also expensive because of the components duplication:

	Quantity	Price	Total
<i>CW DFB Laser</i>	x 2	2.490,00 €	4.980,00 €
<i>EDFA</i>	x 2	3.690,00 €	7.380,00 €
<i>PC</i>	x 2	166,15 €	332,30 €
<i>MZM</i>	x 2	1.998,00 €	3.996,00 €
<i>15 GHz Oscillator</i>	x 2	36,73 €	73,46 €
<i>DC Source</i>	x 2	988,71 €	1.977,42 €
<i>OBPF</i>	x 2	84,75 €	169,50 €
<i>Optical coupler</i>	x 1	3,86 €	7,72 €
<i>Total</i>			18.916,40 €

Table 7. Estimated budget for the system from section 4.6

Chapter 6. Conclusions and Future Lines

6.1 Conclusions

In this thesis, several RF mm-wave signal generation systems have been proposed and simulated. The simulation and analysis emerge different conclusions:

- After showing a conventional mm-wave data transmission RoF system, an alternative design based on MWP techniques has been demonstrated. Both are able to transmit up to 10 Gbps and the mm-wave carriers generated have a similar quality. However, from the point of view of the data transmission performance and the equipment cost, the MWP based design is recognised as a better option.
- Besides, the successful performance of the MWP based design, it has the economic advantage of employing an oscillator with the half frequency than the other design. In such high frequency levels, the oscillator's price rises considerably. So, it has a really satisfactory performance with a lesser economic impact.
- An additional generator system based on the same MWP principle as the alternative transmission design is simulated. It also employs a frequency shift module based on the SBS effect to increase the generated carrier frequency without employing a higher frequency oscillator. Therefore, it allows higher frequency RF mm-wave signal generation without incurring in more expensive oscillators and a better tunability performance by not only enabling to tune the signal frequency with the frequency driven the MZM but also by benefiting from the SBS characteristics of the fiber employed.
- Microwave photonic techniques together with SBS effect can not only generate high frequency signals but also build triangular-shaped high frequency pulses as demonstrated. Making use of the techniques explained, an only odd-order harmonics signal is produced. It contains only two odd-order harmonics but they are enough.
- A design based on the OCS method but employing two lasers is introduced to provide an enhanced flexibility. By utilizing two lasers with different emission frequency, modulating them with MZM driven with distinct frequencies and filtering the sidebands desired a more flexible system is achieved. The higher cost generated by the employment of two lasers is compensated by the flexibility provided.
- Lastly but not least, the higher cost from the last three designs is compensated by its contributions. Besides, the studies are still immature and must be deeply investigated before discarding them.

6.2 Future Lines

Once the work is finalized, some future research lines can be identified whether through the difficulties presented with the simulation platform software or their interest. The proposed future research areas are:

- Test the data transmission in every scheme presented. Not only is important the quality of the carrier generated but also if it is suitable for data transmission.
- Study the systems performance when employing different modulation format. It hasn't been done in this thesis due to the problems obtained when trying N-QAM data transmitting.
- Feasibility of using a Fabry-Perot laser instead of two DFB lasers in the last design. If two spectral lines of the laser can be filtered and modulated through a MZM, a similar behaviour could be reached without incurring in the higher cost of utilizing two lasers. However, as the spectral lines are not completely independent, the system should be deeply studied.
- Study and improvement of the design proposed in section 4.6.
- Once the theoretical and simulation work is realized is especially important to check the experimental behaviour. So, the experimental study is left to subsequent researches.
- The combined operation of RF mm-wave signal generation with optical conformation systems is an area still to investigate.

References

- [1] X. Hou, X. Wang, H. Jiang, and H. Kayama, "Investigation of Massive MIMO in Dense Small Cell Deployment for 5G," in *Vehicular Technology Conference (VTC-Fall), 2016 IEEE 84th*, 2016, pp. 1–6.
- [2] G. Liu *et al.*, "3-D-MIMO With Massive Antennas Paves the Way to 5G Enhanced Mobile Broadband: From System Design to Field Trials," *IEEE J. Sel. Areas Commun.*, vol. 35, no. 6, pp. 1222–1233, Jun. 2017.
- [3] L. Wan, M. Zhou, and R. Wen, "Evolving LTE with flexible duplex," in *Globecom Workshops (GC Wkshps), 2013 IEEE*, 2013, pp. 49–54.
- [4] P. Pirinen, "Challenges and possibilities for flexible duplexing in 5G networks," in *Computer Aided Modelling and Design of Communication Links and Networks (CAMAD), 2015 IEEE 20th International Workshop on*, 2015, pp. 6–10.
- [5] U. Siddique, H. Tabassum, E. Hossain, and D. I. Kim, "Wireless backhauling of 5G small cells: Challenges and solution approaches," *IEEE Wirel. Commun.*, vol. 22, no. 5, pp. 22–31, 2015.
- [6] R.-A. Pitaval, O. Tirkkonen, R. Wichman, K. Pajukoski, E. Lahetkangas, and E. Tirola, "Full-duplex self-backhauling for small-cell 5G networks," *IEEE Wirel. Commun.*, vol. 22, no. 5, pp. 83–89, 2015.
- [7] S. Samarakoon, M. Bennis, W. Saad, and M. Latva-aho, "Backhaul-Aware Interference Management in the Uplink of Wireless Small Cell Networks," *IEEE Trans. Wirel. Commun.*, vol. 12, no. 11, pp. 5813–5825, Nov. 2013.
- [8] X. Shen, "Device-to-device communication in 5G cellular networks," *IEEE Netw.*, vol. 29, no. 2, pp. 2–3, 2015.
- [9] K. Doppler, M. Rinne, C. Wijting, C. B. Ribeiro, and K. Hugl, "Device-to-device communication as an underlay to LTE-advanced networks," *IEEE Commun. Mag.*, vol. 47, no. 12, 2009.
- [10] P. Janis, V. Koivunen, C. Ribeiro, J. Korhonen, K. Doppler, and K. Hugl, "Interference-aware resource allocation for device-to-device radio underlaying cellular networks," in *Vehicular Technology Conference, 2009. VTC Spring 2009. IEEE 69th*, 2009, pp. 1–5.
- [11] Y.-L. Chung, "A study of advanced D2D transmission for use in 5G cellular systems," in *Information Networking (ICOIN), 2017 International Conference on*, 2017, pp. 298–302.
- [12] N. Alliance, "5G white paper," *Gener. Mob. Netw. White Pap.*, 2015.
- [13] Ericsson, "5G Radio Access: Technology and Capabilities," *White Pap.*, Feb. 2015.
- [14] S. Tombaz, P. Frenger, F. Athley, E. Semaan, C. Tidestav, and A. Furuskar, "Energy Performance of 5G-NX Wireless Access Utilizing Massive Beamforming and an Ultra-Lean System Design," 2014, pp. 1–7.
- [15] G.-K. Chang and C. Liu, "1–100GHz microwave photonics link technologies for next-generation WiFi and 5G wireless communications," in *Microwave Photonics (MWP), 2013 International Topical Meeting on*, 2013, pp. 5–8.
- [16] R. Waterhouse and D. Novack, "Realizing 5G: Microwave Photonics for 5G Mobile Wireless Systems," *IEEE Microw. Mag.*, vol. 16, no. 8, pp. 84–92, Sep. 2015.
- [17] M. Talwar, "5G Network a Zero Distance Connectivity Between People," *Int. J. Emerg. Technol.*, vol. 6, no. 1, p. 110, 2015.
- [18] S. Methley, W. Webb, S. Walker, and J. Parker, "5G Candidate Band Study." Quotient Associates, Mar-2015.

- [19]FCC, “FCC Spectrum Frontiers (mmW) Order on 28373964-71GHz and Further Notice of Proposed Rulemaking (FNPRM).” 14-Jul-2016.
- [20]“Framework and overall objectives of the future development of IMT for 2020 and beyond,” Recommendation ITU-R M-2083-0, Sep. 2015.
- [21]“Studies on frequency-related matters for International Mobile Telecommunications identification including possible additional allocations to the mobile services on a primary basis in portion(s) of the frequency range between 24.25 and 86 GHz for the future development of International Mobile Telecommunications for 2020 and beyond,” Resolution Resolution 238 (WRC-15), Nov. 2015.
- [22]ITU-R, “Minimum requirements related to technical performance for IMT-2020 radio interface(s),” IMT-2020.TECH PERF REQ, Feb. 2017.
- [23]K. Xu *et al.*, “Microwave photonics: radio-over-fiber links, systems, and applications [Invited],” *Photonics Res.*, vol. 2, no. 4, p. B54, Aug. 2014.
- [24]C. H. Cox, *Analog Optical Links: Theory and Practice*. Cambridge University Press, 2006.
- [25]Z. Cao, “Radio beam steering in indoor fibre-wireless networks,” *Power DBm*, vol. 20, no. 10, p. 0, 2015.
- [26]X. Liu *et al.*, “Photonic Generation of Triangular-Shaped Microwave Pulses Using SBS-Based Optical Carrier Processing,” *J. Light. Technol.*, vol. 32, no. 20, pp. 3797–3802, Oct. 2014.
- [27]F. Xin, J. Yan, and Q. Liu, “An Optical Microwave Generator based on Stimulated Brillouin Scattering with Fine Tunability,” *Sch. Electron. Inf. Eng. Beihang Univ. Beijing China*.
- [28]Huanfa Peng *et al.*, “Tunable DC-60 GHz RF Generation Utilizing a Dual-Loop Optoelectronic Oscillator Based on Stimulated Brillouin Scattering,” *J. Light. Technol.*, vol. 33, no. 13, pp. 2707–2715, Jul. 2015.
- [29]Chung-Yu Lin, Yu-Chieh Chi, Cheng-Tin Tsai, Huai-Yung Wang, and Gong-Ru Lin, “39-GHz Millimeter-Wave Carrier Generation in Dual-Mode Colorless Laser Diode for OFDM-MMWoF Transmission,” *IEEE J. Sel. Top. Quantum Electron.*, vol. 21, no. 6, pp. 609–618, Nov. 2015.
- [30]W. Roh *et al.*, “Millimeter-wave beamforming as an enabling technology for 5G cellular communications: theoretical feasibility and prototype results,” *IEEE Commun. Mag.*, vol. 52, no. 2, pp. 106–113, 2014.
- [31]Z. Cao, X. Zhao, F. M. Soares, N. Tessema, and A. M. J. Koonen, “38-GHz Millimeter Wave Beam Steered Fiber Wireless Systems for 5G Indoor Coverage: Architectures, Devices, and Links,” *IEEE J. Quantum Electron.*, vol. 53, no. 1, pp. 1–9, Feb. 2017.
- [32]J. Capmany, B. Ortega, and D. Pastor, “A tutorial on microwave photonic filters,” *J. Light. Technol.*, vol. 24, no. 1, pp. 201–229, Jan. 2006.
- [33]J. Zhang, J. Yu, N. Chi, F. Li, and X. Li, “Experimental demonstration of 24-Gb/s CAP-64QAM radio-over-fiber system over 40-GHz mm-wave fiber-wireless transmission,” *Opt. Express*, vol. 21, no. 22, p. 26888, Nov. 2013.
- [34]M. Weiß, M. Huchard, A. Stohr, B. Charbonnier, S. Fedderwitz, and D. S. Jager, “60-GHz Photonic Millimeter-Wave Link for Short- to Medium-Range Wireless Transmission Up to 12.5 Gb/s,” *J. Light. Technol.*, vol. 26, no. 15, pp. 2424–2429, Aug. 2008.
- [35]“Thorlabs, Inc. - Your Source for Fiber Optics, Laser Diodes, Optical Instrumentation and Polarization Measurement & Control,” *Thorlabs, Inc. - Your Source for Fiber Optics, Laser Diodes, Optical Instrumentation and Polarization Measurement & Control*. [Online]. Available: <http://www.thorlabs.com>. [Accessed: 11-Sep-2017].

- [36]“DigiKey Electronics - Electronic Components Distributor.” [Online]. Available: <http://www.digikey.com>. [Accessed: 11-Sep-2017].
- [37]“Mouser Electronics Spain - Electronic Components Distributor.” [Online]. Available: <http://www.mouser.com>. [Accessed: 11-Sep-2017].